

EFFECT OF OVALITENONE ON NON-SMALL CELL LUNG CANCER CELLS



A Thesis Submitted in Partial Fulfillment of the Requirements  
for the Degree of Master of Science in Pharmacology  
Inter-Department of Pharmacology  
GRADUATE SCHOOL  
Chulalongkorn University  
Academic Year 2020  
Copyright of Chulalongkorn University

ผลของสารโอวาริตินต่อเซลล์มะเร็งปอดชนิดไม่ใช้เซลล์เล็ก



วิทยานิพนธ์นี้เป็นส่วนหนึ่งของการศึกษาตามหลักสูตรปริญญาวิทยาศาสตรมหาบัณฑิต  
สาขาวิชาเภสัชวิทยา สหสาขาวิชาเภสัชวิทยา  
บัณฑิตวิทยาลัย จุฬาลงกรณ์มหาวิทยาลัย  
ปีการศึกษา 2563  
ลิขสิทธิ์ของจุฬาลงกรณ์มหาวิทยาลัย



กิตติพงษ์ สนุกพันธ์ : ผลของสารโอวาริตินอนต่อเซลล์มะเร็งปอดชนิดไม่ใช่เซลล์เล็ก. ( EFFECT OF OVALITENONE ON NON-SMALL CELL LUNG CANCER CELLS) อ.ที่ปรึกษาหลัก : ศ. ภก. ดร.ปิ ตี จันทรรวัชโชติ

การแพร่กระจายของมะเร็งเป็นสาเหตุสำคัญของการเสียชีวิตจากมะเร็งประมาณร้อยละ 90 และการเปลี่ยนแปลงลักษณะของเซลล์เยื่อบุผิวไปเป็นเซลล์มีเซนไคม์ (epithelial-to-mesenchymal transition หรือ EMT) เป็นอีกบทบาทสำคัญอย่างหนึ่งที่เกี่ยวข้องในการแพร่กระจายของเซลล์มะเร็ง ดังนั้นในการศึกษานี้มีวัตถุประสงค์เพื่อศึกษาผลของสารโอวาริตินอนต่อการยับยั้งการเปลี่ยนแปลงลักษณะของเซลล์เยื่อบุผิวไปเป็นเซลล์มีเซนไคม์ และยับยั้งพฤติกรรมที่เกี่ยวข้องกับการแพร่กระจายของเซลล์มะเร็ง เช่น การเคลื่อนที่ (migration) การเจริญเติบโตในสภาวะไร้ที่ยึดเกาะ (anchorage-independent growth) และเซลล์มะเร็งต้นกำเนิด (cancer stem cells หรือ CSCs) ของเซลล์มะเร็งปอด สารโอวาริตินอนเป็นฟลาโวนอยด์ที่สกัดจากรากของ *Millettia erythrocalyx* Gapnep. ถูกรายงานครั้งแรกว่ามีฤทธิ์ในการยับยั้งการเคลื่อนที่ของเซลล์มะเร็งปอดชนิด H460 และ A549 สารโอวาริตินอนถูกใช้ที่ความเข้มข้น 0–200 ไมโครโมลาร์ ( $\mu\text{M}$ ) ซึ่งไม่ก่อให้เกิดความเป็นพิษต่อเซลล์มะเร็งปอดชนิด H460 และ A549 และยังสามารถยับยั้งการเจริญเติบโตแบบที่ไม่ต้องอาศัยเซลล์ยึดเกาะ การแสดงออกเสมือนเซลล์ต้นกำเนิด (CSC-like phenotypes) การสร้างโคโลนี (colony formation) ความสามารถในการเคลื่อนที่ และรุกรานของเซลล์มะเร็งปอด ผลในการยับยั้งการเคลื่อนที่ถูกยืนยันโดยการลดลงของจำนวน filopodia ในเซลล์ที่ได้รับสารโอวาริตินอน และยังพบว่าสารโอวาริตินอนสามารถเพิ่มระดับของ E-cadherin ในขณะที่สามารถลดระดับของ N-cadherin, Snail และ Slug ได้อย่างมีนัยสำคัญทางสถิติ ซึ่งบ่งบอกถึงการยับยั้งการทำงานของ EMT นอกจากนี้ โปรตีนไคเนส บี (AKT) และ mammalian target of rapamycin (mTOR) ยังถูกยับยั้งโดยสารโอวาริตินอน ในผลการวิจัยนี้ชี้ให้เห็นว่าสารโอวาริตินอนสามารถลด EMT ผ่านการยับยั้ง AKT/mTOR นอกจากนี้ สารโอวาริตินอนยังแสดงศักยภาพในการยับยั้ง CSC phenotypes จากการศึกษาที่ได้กล่าวมานี้เป็นหลักฐานสนับสนุนให้สารโอวาริตินอนสามารถเป็นสารใหม่ที่มีประสิทธิภาพในการพัฒนาเพื่อรักษามะเร็งปอดต่อไป

สาขาวิชา      เภสัชวิทยา  
ปีการศึกษา      2563

ลายมือชื่อนิสิต .....  
ลายมือชื่อ อ.ที่ปรึกษาหลัก .....

# # 6280112920 : MAJOR PHARMACOLOGY

KEYWORD: Ovalitenone, metastasis, migration, epithelial-mesenchymal transition (EMT),  
lung cancer

Kittipong Sanookpan : EFFECT OF OVALITENONE ON NON-SMALL CELL LUNG CANCER  
CELLS. Advisor: Prof. PITHI CHANVORACHOTE, Ph.D.

Cancer metastasis is the major cause of about 90% of cancer deaths. As epithelial-to-mesenchymal transition (EMT) is known for potentiating metastasis. In the present study aimed to elucidate the effect of ovalitenone on the suppression of EMT and metastasis-related behaviors, including cell movement and growth under detached conditions, and cancer stem cells (CSCs), of lung cancer cells. Ovalitenone, as a flavonoid was extracted from roots of *Millettia erythrocalyx* Gapnep., was the first reported to show the anti-migration activity of H460 and A549 lung cancer cells. Ovalitenone was used at concentrations of 0–200  $\mu\text{M}$ . While it caused no cytotoxic effects on lung cancer H460 and A549 cells, ovalitenone significantly suppressed anchorage-independent growth, CSC-like phenotypes, colony formation, as well as the ability of the cancer to migrate and invade cells. The anti-migration activity was confirmed by the reduction of filopodia in the cells treated with ovalitenone. Interestingly, we found that ovalitenone could significantly increase the level of E-cadherin, whereas it decreases the levels of N-cadherin, Snail, and Slug, indicating EMT suppression. Additionally, ATP-dependent tyrosine kinase (AKT), and the mammalian target of rapamycin (mTOR) were suppressed by ovalitenone. The results suggest that ovalitenone suppresses EMT via suppression of the AKT/mTOR signaling pathway. Furthermore, ovalitenone exhibited potential for the suppression of CSC phenotypes. These data reveal the anti-metastasis potential of the compound and support the development of ovalitenone treatment for lung cancer therapy.

Field of Study: Pharmacology

Student's Signature .....

Academic Year: 2020

Advisor's Signature .....

## ACKNOWLEDGEMENTS

Firstly, I would like to my deepest appreciation to Professor Pithi Chanvorachote, Ph.D. as my advisor for valuable advice, professional advice, excellent support and encouragement throughout every stage of your studies. Without his kindness and understanding, this work could not be accomplished.

Special thanks to Associated Professor Boonchoo Sritularak, Ph.D. for providing ovalitenone from his laboratory for use in this study.

I would like to thank Nongyao Nonpanya, Ph.D. as Postdoctoral researcher in my laboratory for valuable assistance in many aspects.

Finally, I would like to express my deepest gratitude to my parents for their understanding, support and encouragement during my education.

Kittipong Sanookpan

## TABLE OF CONTENTS

	Page
ABSTRACT (THAI).....	iii
ABSTRACT (ENGLISH).....	iv
ACKNOWLEDGEMENTS.....	v
TABLE OF CONTENTS.....	vi
LIST OF TABLES.....	ix
LIST OF FIGURES.....	x
CHAPTER I.....	1
INTRODUCTION.....	1
1.1 Background and rationale.....	1
1.2 Objectives.....	4
1.3 Hypothesis.....	4
1.4 Conceptual framework.....	4
1.5 Research design.....	5
CHAPTER II.....	6
LITERATURE REVIEWS.....	6
2.1 Lung cancer.....	6
2.1.1 Types of lung cancer.....	6
2.1.2 Risk factors.....	7
2.1.3 Stages of lung cancer.....	8
2.1.4 Symptoms of lung cancer.....	8
2.1.5 Treatment for lung cancer.....	9

2.2 Cancer Metastasis.....	9
2.2.1 Migration .....	10
2.2.2 Invasion .....	10
2.2.3 Proteins regulate migration and invasion.....	11
2.3 Epithelial-mesenchymal transition (EMT).....	15
2.3.1 Molecular mechanisms of EMT.....	16
2.3.2 EMT and signaling pathways.....	16
2.3.3 Transcriptional regulation of EMT .....	17
2.3.4 Crosstalk of signaling pathways in EMT.....	17
2.4 Phytochemical .....	19
CHAPTER III.....	20
MATERIALS AND METHODS .....	20
3.1 Chemicals.....	20
3.2 Test compound .....	21
3.3 Cell culture.....	21
3.4 Methods .....	22
3.4.1 Cell viability and cell proliferation assay.....	22
3.4.2 Nuclear staining assay .....	22
3.4.3 Apoptosis assay .....	23
3.4.4 Colony formation assay.....	23
3.4.5 Migration assay .....	24
3.4.6 Cell morphology and filopodia characterization.....	24
3.4.7 Invasion assay .....	25
3.4.8 Anchorage-independent growth assay .....	26



3.4.9 Spheroid formation assay.....	26
3.4.10 Western blot Analysis .....	27
3.4.11 Immunofluorescence assay.....	27
3.5 Statistical analysis.....	28
CHAPTER IV .....	29
RESULTS.....	29
4.1 Effect of ovalitenone on cell viability and proliferation of H460 and A549 cells .....	29
4.2 Effect of ovalitenone on lung cancer cell migration, invasion and filopodia formation.....	35
4.3. Ovalitenone attenuates anchorage-independent growth and CSC-like phenotypes of human lung cancer H460 and A549 cells.....	39
4.4. Ovalitenone suppresses EMT via the suppression of the AKT/mTOR signalling pathway .....	43
CHAPTER IV .....	55
DISCUSSION AND CONCLUSION .....	55
APPENDIX.....	61
REFERENCES .....	64
VITA.....	75

## LIST OF TABLES

	Page
Table 1 Chemicals compound.....	19



## LIST OF FIGURES

	Page
Figure 1 Histologic subtypes of non-small lung cancers.....	6
Figure 2 Step of cancer invasion and metastasis.....	10
Figure 3 Focal adhesion kinase pathway.....	12
Figure 4 Schematic of connections between AKT and metastasis.....	13
Figure 5 The mammalian target of rapamycin complexes and signaling pathway.....	14
Figure 6 Schematic of the signal transduction pathways associate with EMT.....	16
Figure 7 Signaling pathways involved in EMT.....	18
Figure 8 Structure of ovalitenone.....	19
Figure 9 Effect of ovalitenone on cell viability of H460 and A549 cells.....	29
Figure 10 Effect of ovalitenone on cell proliferation of H460 and A549 cells.....	30
Figure 11 Apoptosis effect of ovalitenone on H460 and A549 cells.....	31
Figure 12 Effect of ovalitenone on apoptosis by flow cytometry in H460 cells.....	32
Figure 13 Effect of ovalitenone on apoptosis by flow cytometry of A549 cells.....	33
Figure 14 Effect of ovalitenone on cell proliferation by colony formation assay in H460 and A549 cells.....	34
Figure 15 Ovalitenone suppressed cell migration in H460 and A549 cells.....	36
Figure 16 Ovalitenone suppressed cell invasion in H460 and A549 cells.....	37
Figure 17 Ovalitenone suppressed filopodia formation in H460 and A549 cells.....	38
Figure 18 Ovalitenone attenuates anchorage-independent growth of H460 and A549 cells.....	40
Figure 19 Ovalitenone attenuates cancer stem cell (CSC)-like phenotypes of H460 cells.....	41

Figure 20 Ovalitenone attenuates cancer stem cell (CSC)-like phenotypes of A549 cells.....	42
Figure 21 Effect of ovalitenone on epithelial-to-mesenchymal transition (EMT) markers in H460 cells.....	44
Figure 22 Effect of ovalitenone on epithelial-to-mesenchymal transition (EMT) markers in A549 cells.....	45
Figure 23 Ovalitenone suppresses epithelial-to-mesenchymal transition (EMT) through inhibition of the ATP-dependent tyrosine kinase (AKT)/mammalian target of rapamycin (mTOR) signaling pathway in H460 cells.....	47
Figure 24 Ovalitenone suppresses epithelial-to-mesenchymal transition (EMT) through inhibition of the ATP-dependent tyrosine kinase (AKT)/mammalian target of rapamycin (mTOR) signaling pathway in A549 cells.....	48
Figure 25 Ovalitenone increase E-cadherin in H460 cells.....	49
Figure 26 Ovalitenone suppress N-cadherin in H460 cells.....	50
Figure 27 Ovalitenone suppress Snail in H460 cells.....	51
Figure 28 Ovalitenone increase E-cadherin in A549 cells.....	52
Figure 29 Ovalitenone suppress N-cadherin in A549 cells.....	53
Figure 30 Ovalitenone suppress Snail in A549 cells.....	54
Figure 31 The schematic diagram summarizes the underlying mechanism of ovalitenone-attenuating EMT in lung cancer.....	60

# CHAPTER I

## INTRODUCTION

### 1.1 Background and rationale

Lung cancer is the most commonly diagnosed cancer and continues to be the leading cause of cancer-related deaths worldwide <sup>(1),(2)</sup>. Most cancer deaths are caused by cancer metastasis, accounting for approximately 90% of cancer deaths <sup>(3)</sup>. Cancer metastasis is a molecular process of the spread of cancer cells from a primary tumor to a different site of the body through blood and lymphatic vessels <sup>(4)</sup>. During process of metastasis, epithelial–mesenchymal transition (EMT), cell migration, and invasion have been shown to play important roles and have been linked with high metastasis potentials of cancer cells <sup>(5)</sup>. EMT increases the abilities of the cancer cells to enhances migration, invasion, as well as cell survival in anchorage-independent conditions <sup>(6)</sup>. Accordingly, anti-metastatic agents such as small-molecule inhibitors, immunotherapies, integrin inhibitors, MMP inhibitors, and others are often used as assistant agents to cancer therapy <sup>(7)</sup>. Previous studies reported that small-molecule inhibitors such as KTP-6566 and CCG-203971 significantly decreased lung metastasis <sup>(8)</sup>. Currently, even though chemotherapy drugs are able to treat lung cancer but it has a great number of reports to resistance of chemotherapy drugs in some patient's disease <sup>(9)</sup>.

Cancer metastasis is a process of cancer cells spreading into neighboring tissues through the blood or lymph system to other organs <sup>(10)</sup>. Cell migration and invasion are related to cancer metastasis <sup>(11)</sup>. Metastatic cells detach of the tumor cells from the primary tumor site, invade and migrate through the basement membrane (BM) and the extracellular matrix (ECM), enter the blood or lymphatic vessels. One biological

mechanism responsible for cancer metastasis is also known as epithelial to mesenchymal transition (EMT) <sup>(12)</sup>. EMT is not only an essential process in which epithelial cells acquire the motile and invasive phenotype of mesenchymal cells, but also an importance process for anoikis resistance <sup>(13)</sup>. The critical hallmarks of EMT are E-cadherin, N-cadherin, as well as the up-regulation of Vimentin, Slug and Snail proteins <sup>(14)</sup>. N-cadherin up-regulation and E-cadherin down-regulation, also known as cadherin switching, has been found to be the most important marker for EMT, and its associated with increased migratory and invasive behavior <sup>(15)</sup>. Importantly, the loss of E-cadherin-mediated adhesion has been shown to play a significant role in the transition of epithelial cells from a benign to an invasive step. However, the high levels of expression of N-cadherin in invasive cancer cells which was inversely correlated with E-cadherin expression <sup>(16)</sup>. Furthermore, Slug, Snail, and Twist are transcription factors that regulate the level expression E-cadherin <sup>(17)</sup>. These transcription factors act as molecular switch suppressing the expressing of E-cadherin by repressing a set of gene that encodes E-cadherin <sup>(18)</sup>.

Cell migration through tissues results from highly integrated multistep process that are regulated by various signaling molecules such as integrins, Rho-GTPases, and focal adhesion kinase (FAK) <sup>(19), (20), (21)</sup>. Focal adhesion kinase (FAK) is an intracellular protein-tyrosine kinase (PTK) involved in the regulation of cell cycle progression, survival, and migration <sup>(22)</sup>. The ability of cancer cells to migrate has been found to be linked to increased FAK expression, phosphorylation and catalytic activity <sup>(23)</sup>. The phosphorylation of Y397 of FAK plays crucial role in FAK-mediated cell migration <sup>(24)</sup>. In lung cancer, ATP-dependent tyrosine kinase (AKT; also known as protein kinase B) is activated, and increased AKT phosphorylation is associated with cancer metastasis <sup>(25)</sup>.

Many reports have showed that AKT is a down-stream target of FAK<sup>(26)</sup>. Several studies shown that the mammalian target of rapamycin (mTOR) also plays an important role in the regulation of cell migration, invasion and cancer metastasis<sup>(27),(28)</sup>. Moreover, the activation of FAK and its downstream targets such as the Rho family protein and cell division cycle 42 (Cdc42) are also known to regulate cell migration and the formation of filopodia<sup>(29)</sup>. There is potential utility in molecularly targeting components of these signaling pathways for cancer prevention, and cancer therapy.

Consequently, alterations of these molecules could proficiently prevent cancer metastasis. Therefore, the new compounds derived from several type of plants with anti-cancer activities as well as antimetastatic effects would be beneficial for the disease managements. Although chemotherapy is currently used for cancer treatment that uses one or more anti-cancer drugs to destroy cancer cells, this can cause toxic side effects, hair loss, high-dose requirements, damage some healthy cells, as well as the development of drug resistance<sup>(30)</sup>. The failure of standard treatments in the management of cancer metastasis has fueled a revival of research interest in natural resource active compounds<sup>(31)</sup>. Recently, it has been reported that natural plant compounds are receiving increasing attention, whether they are potent drugs or lead compounds in drug discovery<sup>(32)</sup>. *Millettia erythrocalyx* is widely distributed in the tropical and subtropical regions of the world such as China, and Thailand<sup>(33)</sup>. This study focus on the activity of ovalitenone as a flavonoid<sup>(34)</sup>. This compound is also extracted from roots of *M. erythrocalyx* or “Chan” in Thailand<sup>(35)</sup>. Ovalitenone was shown to uses in traditional medicine such as bleeding piles, fistulous sores, bronchitis, and cough<sup>(36)</sup>. Furthermore, it has a great number of process effects such as anti-diabetic activity<sup>(37)</sup>, and anti-herpes simplex virus activity<sup>(38)</sup>; however, the effect of ovalitenone

on metastasis potentials, EMT and underlying mechanisms have not been reported. Therefore, the objective of this study was to investigate the effect of ovalitenone on migration, invasion in lung cancer cells. The results from this study may benefit the development of ovalitenone for anti-metastatic therapy.

## 1.2 Objectives

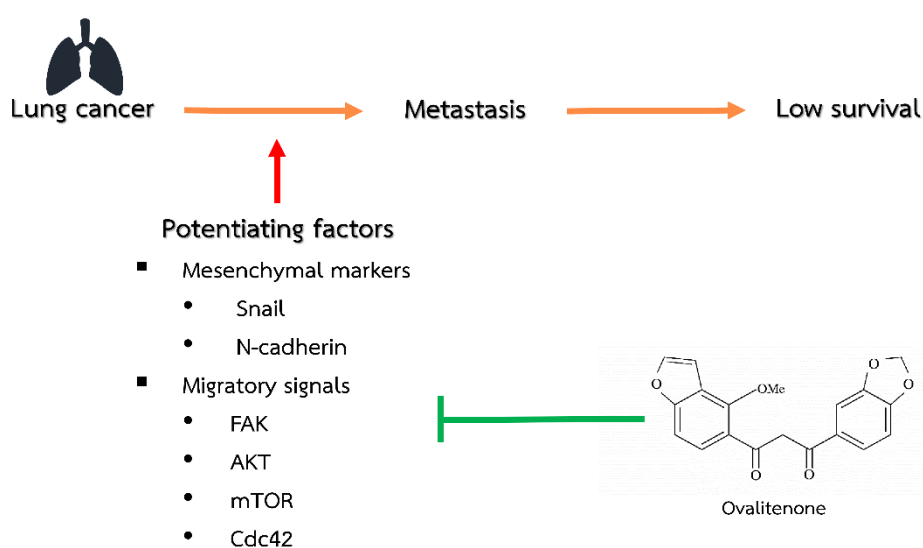
**1.1.1** To investigate the effect of ovalitenone on migration and invasion behaviors of lung cancer cells.

**1.1.2** To investigate the epithelial to mesenchymal transition (EMT) suppressing activity of ovalitenone.

## 1.3 Hypothesis

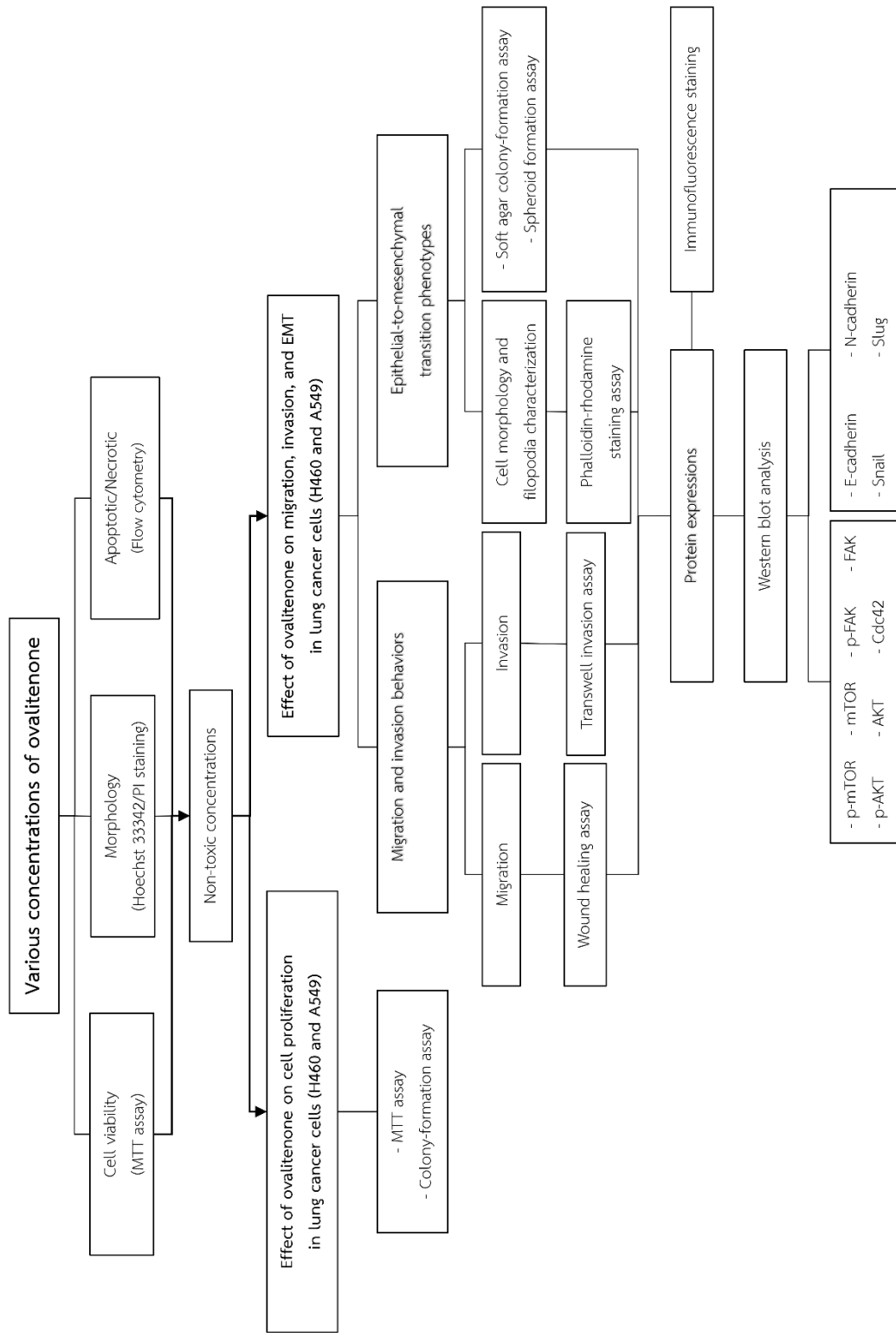
Ovalitenone suppresses migration and invasion of lung cancer cells by suppress EMT and migratory signals such as FAK, AKT/mTOR, Cdc42 signal pathway.

## 1.4 Conceptual framework





## 1.5 Research design



## CHAPTER II

### LITERATURE REVIEWS

#### 2.1 Lung cancer

Lung cancer is often the leading cause of cancer death in both men and women in the world. In 2018, 18.1 million an estimate that will be new cases (17.0 million) and 9.6 million cancer deaths worldwide. Lung cancer is commonly diagnosed in approximately 11.6% of all cases and is the leading cause of cancer deaths for nearly 18.4% of all cancer deaths <sup>(2)</sup>.

##### 2.1.1 Types of lung cancer

According to the World Health Organization (WHO), lung cancers are divided into two major classes based on its biology such as small cell (SCLC) and non-small cell lung cancer (NSCLC), which originates from epithelial cell precursors in the bronchi <sup>(39)</sup>. What's more, NSCLC is further classified into squamous cell carcinoma (approximately 30% of all cancer cases), adenocarcinoma (approximately 40% of all cancers) and large cell carcinoma (almost 10% of all lung cancer). The overall 5-year survival rate has raised over 2.5 decades (approximately 16%) <sup>(40)</sup>.

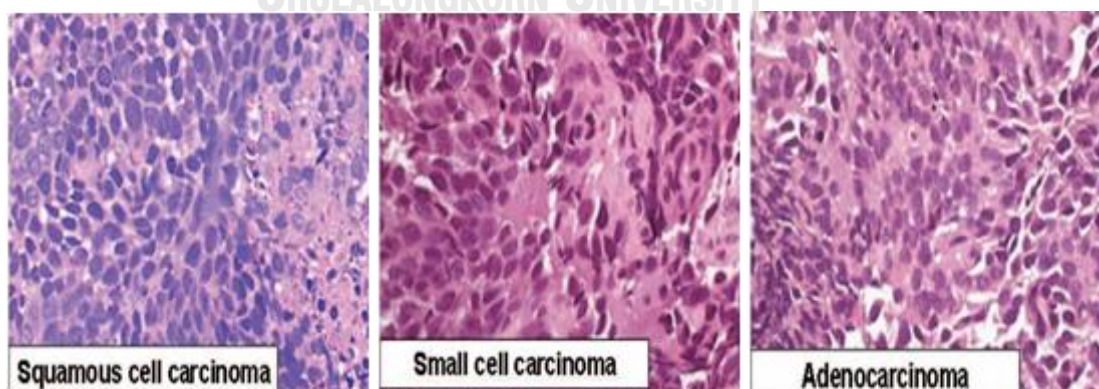


Figure 1 Histologic subtypes of non-small lung cancers

### 2.1.2 Risk factors

The most common lung cancer risk factors are environmental, lifestyle, and occupational exposures. The role of these factors varies, depending on geographic location, gender, race characteristics, and genetic defects are linked to lung cancer.

- Cigarette smoking and Secondhand smoking

Cigarette smoking is the leading cause of lung cancer: around 55% in women and over 70% in men of cancer death on account of smoking. In a cohort study of over 50,000 incident cases of lung cancer between 1 January 1997 and 15 April 2016 reported that there was no evidence of a difference in the risk of lung cancer associated with smoking in women compared to men; however, as smoking prevalence was higher in men greater than women <sup>(42)</sup>.

Secondhand smoking, non-smokers' exposure to cigarette smoke leads to increased concentrations of tobacco-specific carcinogens in both blood and urine. In addition, an excess of 24% lung cancer risk was shown in non-smokers living with a spouse who smoked <sup>(43)</sup>.

- Occupational exposures

Occupational risks play a key role in lung cancer. Two studies report assessing the ratio of representative occupational lung cancer patients in the UK to 14.5% overall and 12.5% in men in France. Furthermore, asbestos, heavy metals, radon, and silica are among the most important lung carcinogens. <sup>(44)</sup>.

- Lung cancer susceptibility genes

Not only exposure to environmental carcinogens, but also host factors that cause lung cancer as well. Segregation studies indicates 2.5-fold the cancer risk from family history. Previous research found that people who have mutation at *K-ras*, or

overexpression of epidermal growth factor receptor (EGFR), cyclin D1, and BCL2 are more promising to develop lung cancer. What's more, mutation of tumor suppressor genes such as p53 is responsible for 50% of non-small cell lung cancers and p16 is responsible for more than 50% of non-small cell lung cancers <sup>(45)</sup>.

### **2.1.3 Stages of lung cancer**

Stages can be used to determine based on the identified tumor types <sup>(46)</sup>. NSCLC is categorized by the TNM (tumor-nodes-metastasis) staging system, where category T describes the extent and size of the primary tumor, category N describes the extent of regional lymph node involvement, and category M describes the presence or absence of peripheral nodes <sup>(47)</sup>.

### **2.1.4 Symptoms of lung cancer**

Symptoms can be caused by the primary tumor such as cough and hemoptysis, while other symptoms such as Horner syndrome and superior vena cava can be caused by the obstruction intrathoracic spread, and bone pain can be caused by distant metastases <sup>(48)</sup>. Previous research longitudinal study of depressive symptoms in patient's lung cancer, 35% of the subjects reported at least mild depression and 16% reported moderate to severe depression <sup>(49)</sup>. Other symptoms of lung cancer are digital clubbing, weight loss, loss of appetite, dyspnea, and fatigue chest or rib pain <sup>(50)</sup>. Moreover, the symptoms in patient's lung cancer occur across different types of tumors <sup>(51)</sup>.

### 2.1.5 Treatment for lung cancer

Cancer treatment aims to eliminate or destroy cancer cells without killing normal cells. There are many ways to cure lung cancer patients such as surgery, radiation, targeted therapy and chemotherapy, which can be used whether alone or combination <sup>(52)</sup>. Firstly, Surgery is by far the best recommend for resect able and operable stage I and II. 5-year survival rates after surgical resection are 77-92% for stage I and 50-60% for stage II <sup>(53)</sup>. In addition to the best choice for treating stage IV patients depends on a number of factors, including radiation therapy, , targeted therapy and combination chemotherapy <sup>(54)</sup>. Even though chemotherapy (cisplatin, taxanes and etoposide) have affected on cancer cells but it has many side effects in some patients such as drug resistance, hematologic toxicity, nephrotoxicity, and nausea and vomiting <sup>(55), (56)</sup>.

### 2.2 Cancer Metastasis

Metastasis is the ability of cancer cells to spread from the original place of cancer to another parts of body. The processes of invasion and metastasis; to begin with cancer cells escape from primary tumor, then cancer cells across the endothelial lamina enter the blood and lymph system (called intravasation), following cancer cells escape from the lamina into parenchyma of distant specific organs (called extravasation). In the end, proliferating from micrometastatic to macrometastatic, which the last step called “colonization” <sup>(57)</sup>. The step of cancer invasion and metastasis, as figure 2.

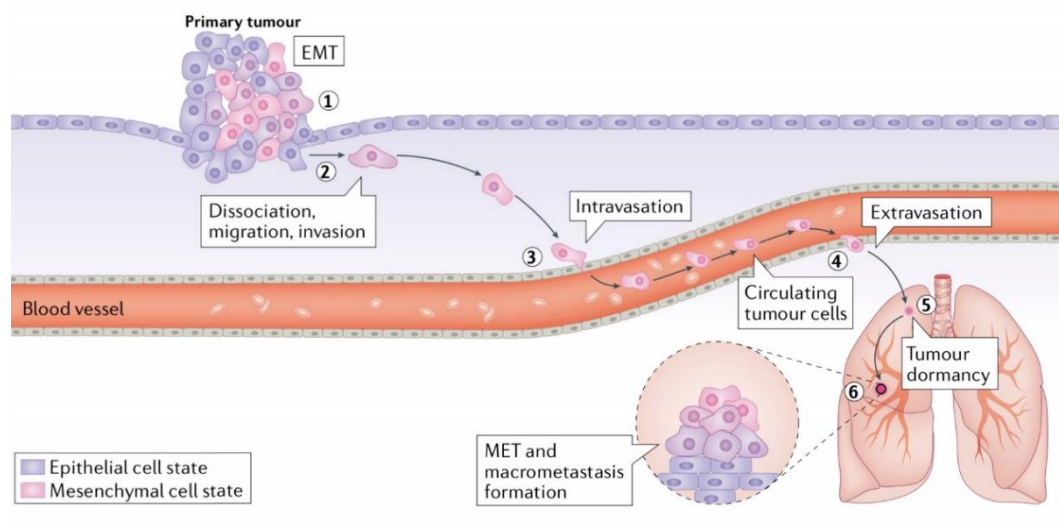


Figure 2 Step of cancer invasion and metastasis

(58)

### 2.2.1 Migration

Cell migration is a basic multi-step process that involves the movement of cells from one part to another. It is an important part of biological phenomena in normal and pathological events <sup>(59)</sup>. It is possible that the better understanding of molecular mechanisms regulating metastasis should lead to the development of new treatment options. Such mechanisms of metastasis and metastatic factors include growth factor, cytokine, adhesion molecules and proteases should be focused for further investigations <sup>(60), (61)</sup>.

### 2.2.2 Invasion

Invasion is the movement of cancer cells through a nearby extracellular matrix and surrounding. It is generally different from metastasis, which is the spread of cancer cells through the circulatory or lymphatic systems to distant locations <sup>(62)</sup>.

## 2.2.3 Proteins regulate migration and invasion

### 2.2.3.1 Focal adhesion kinase (FAK)

Focal adhesion kinase (FAK) is a 125 kDa cytoplasmic tyrosine kinase which plays an important role in cell skeletal formation and cell adhesion formation. It consists of three domains: the central kinase domain, the N-terminal FERM domain, and the C-terminal focus adhesion target domain. The tyrosine 397 (Tyr397) site of FAK N-terminal domain are known to be phosphorylated causing the active form of FAK. Tyr397 of FAK was shown to be added to autoactivated via autophosphorylation <sup>(63)</sup>. Then, FAK recruits and activates other proteins at the focal adhesion <sup>(64)</sup>. The overexpression of FAK was shown to show the metastatic phenotype of cancer cells by promoting cell migration and invasion. Several studies also found that FAK and phosphorylated FAK (p-FAK) were involved in carcinogenicity <sup>(65)</sup>. In particular, the p-FAK expression is found in many cancers such as lung cancer <sup>(66)</sup>. Several reasonable studies have identified a key role for FAK in regulating cell movement. Interestingly, knockdown of FAK shows slow cellular diffusion on extracellular matrix proteins, cumulative numbers of apparent focal exposure, as well as slow translocation processes in both hepatotactic and chemotactic attraction responses <sup>(67), (68)</sup>.

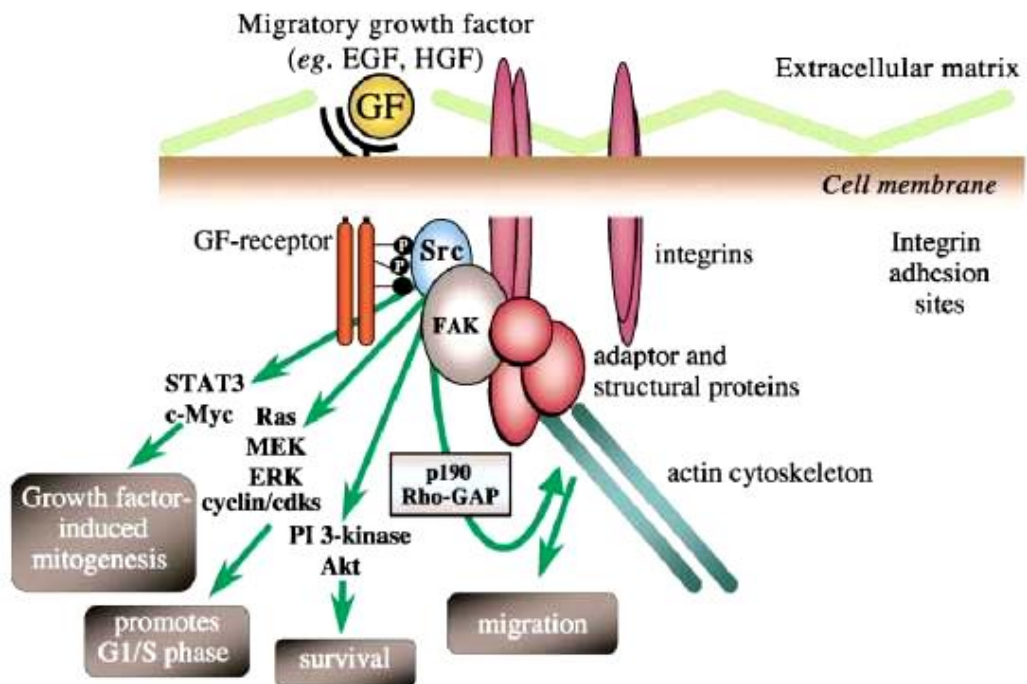


Figure 3 Focal adhesion kinase pathway

(69)

### 2.2.3.2 Protein kinase B (AKT)

Protein kinase B is a downstream of the PI3K signaling. can be stimulated by various growth factors or cytokines. AKT is stimulated to regulate many essential functions of the cell including cell proliferation, cell growth, survivability of cells and aspects of intermediary metabolism<sup>(70)</sup>. AKT was shown to regulate cell migration. The study of AKT in squamous cell carcinoma showed that AKT promotes EMT that results in increased motility and invasion<sup>(71)</sup>. Moreover, AKT play a role in controlling microtubule stability<sup>(72)</sup>. Active AKT (p-AKT) stimulates cell survival to induce proliferation, invasion and metastasis. p-AKT stimulates expression of B-cell lymphoma-2 (Bcl-2) proteins that resist apoptosis while inhibiting the pro-apoptotic Bad, Bax, Bid, and Bim proteins<sup>(73)</sup>. It also showed a significant increase in the AKT trajectory of patients with NSCLC. In the study of 110 NSCLC tumors, 51% were found to be due to an increase in AKT activity<sup>(74)</sup>.



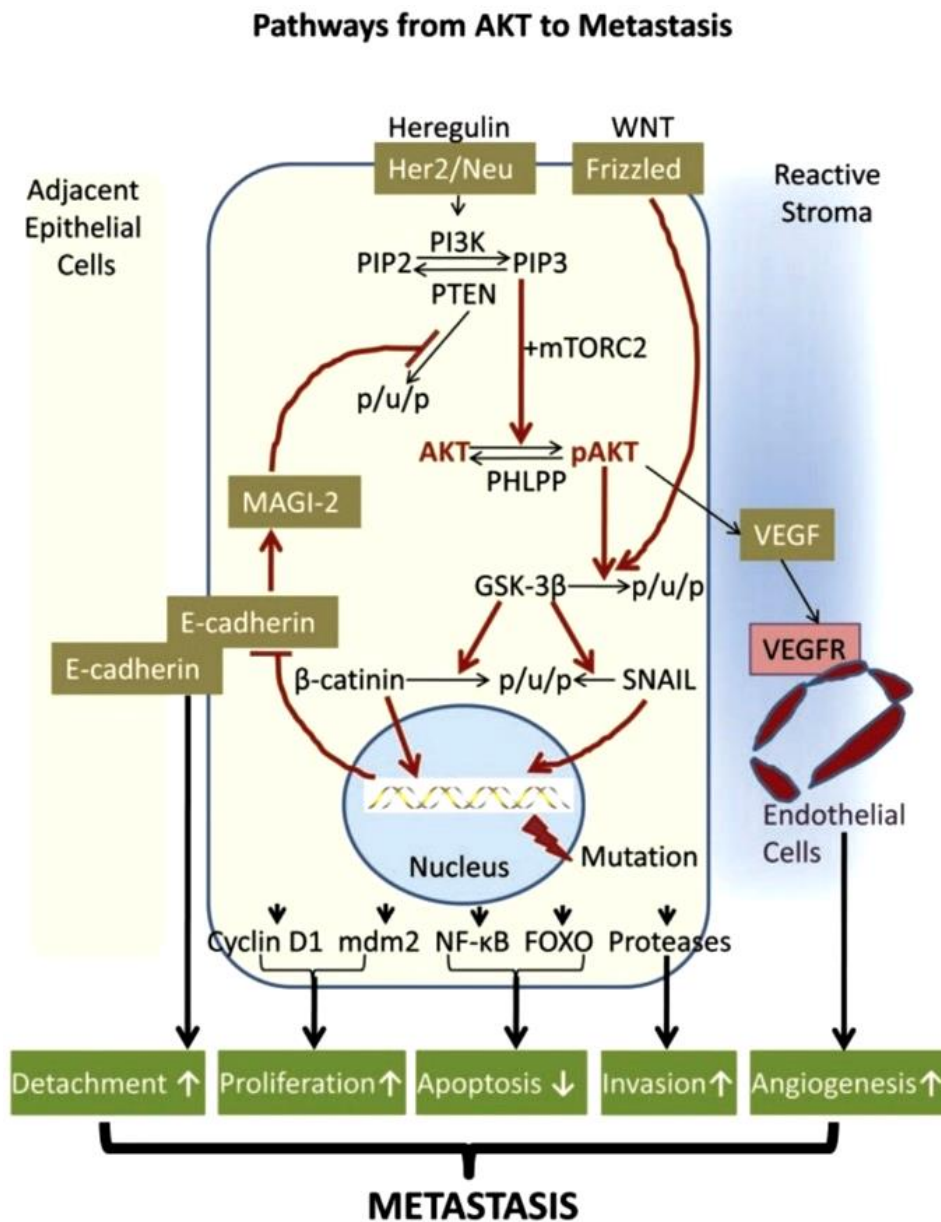


Figure 4 Schematic of connections between AKT and metastasis

(75)

### 2.2.3.3 The mammalian target of rapamycin (mTOR)

The mammalian target of rapamycin (mTOR), a serine/threonine kinase, functions through two of protein complexes; mTOR complex 1 (mTORC1) and mTOR complex 2 (mTORC2). mTOR main function is to sense and integrate intracellular and environmental signals. mTOR signaling is generally involved in regulating cell survival

and growth, cell metabolism, protein synthesis, and autophagy<sup>(76)</sup>. The pathological relevance of the mTOR signal disorder has been demonstrated in many human diseases, particularly many human cancers. According to the report, mTOR has been overused in more than 70% of cancers in recent years. It has been widely shown in animal models and cancer patients that mTOR abnormalities are causing tumors<sup>(77)</sup>. Deregulation of PI3K/AKT/mTOR pathway is involved in lung tumorigenesis and it has also been associated with high grade tumors<sup>(78)</sup>. In addition, upregulation of the mTOR pathway was also demonstrated in a significant proportion of NSCLC tumors, with an increase p-mTOR in up to 90% of adenocarcinomas, 60% of large cell carcinomas and 40% of patients with squamous cell carcinomas<sup>(74)</sup>.

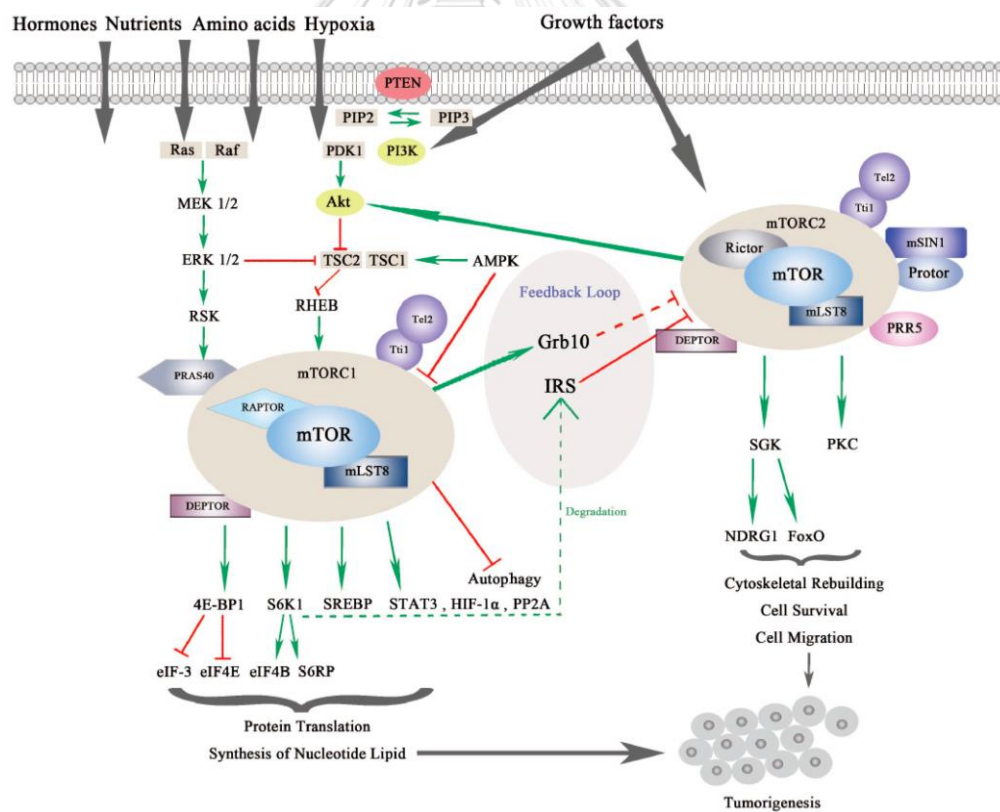


Figure 5 The mammalian target of rapamycin complexes and signaling pathway

(77)

#### 2.2.3.4 Cell division cycle 42 (Cdc42)

Cdc42 is a member of the small GTPase of the Rho family that has multiple regulatory functions for cell skeletal organization, intercellular communication for many physiological steps such as cell proliferation, migration, invasion as well as control of cell direction <sup>(29)</sup>. Cdc42 can be activated by guanine nucleotide exchange factors or GEFs which exchange GDP (guanosine diphosphate)-Cdc42 form to GTP (guanosine triphosphate)-Cdc42 form for Cdc42 stimulation <sup>(79)</sup>. The up-regulation of Cdc42 signals may impair c-Cbl-mediated EGFR degradation, and induce proteasomal degradation of p21CIP1 leading to an increase in cell proliferation and migration, while downregulation of Cdc42 signals can also inhibit anchorage-independent growth and induce apoptosis via the PI(3)K-AKT and ERK signaling cascades <sup>(80)</sup>. Numerous studies, showing that the motility of cancer is associated with overexpression of Cdc42 <sup>(81)</sup>.

### 2.3 Epithelial-mesenchymal transition (EMT)

Epithelial-mesenchymal transition (EMT) is one of the hallmarks of cancer invasion and metastasis that associated cancer cells developed alterations in their shape as well as in their attachment to other cells and to the extracellular matrix (ECM) <sup>(82)</sup>. Generally, the phenomenon of EMT divided into 3 classes: class 1 EMT during embryogenesis and organ development, class 2 is EMT associated with tissue regeneration, and class 3 is involved with cancer invasion and migration <sup>(83)</sup>. Disruption of cell-cell adhesion, apico-basal polar depletion and matrix change may be caused by EMT, resulting in increased motility and invasiveness in tumors metastasis <sup>(84)</sup>.

### 2.3.1 Molecular mechanisms of EMT

During EMT, the characteristic is change from epithelial cells to motile, invasive and migratory mesenchymal cells <sup>(85)</sup>. In these processes, epithelial cells lose cell adhesion, cell polarity, and reducing the expression of epithelial markers such as E-cadherin, while increasing the expression of mesenchymal cell markers such as Vimentin, N-cadherin, Twist, Snail <sup>(86)</sup>.

### 2.3.2 EMT and signaling pathways

EMT can be induced by several intracellular signaling pathways, including TGF- $\beta$  growth factors, Notch, Wnt/ $\beta$ -catenin and Hedgehog pathway, which TGF- $\beta$  is a major inducer of EMT <sup>(87)</sup>. For example, TGF- $\beta$  binds to the receptor and causes the activation of Smad2 and Smad3 via phosphorylation. Activated Smad2 and Smad3 then form trimers with Smad4 resulting in Smad complex that translocate to nucleus <sup>(86)</sup>.

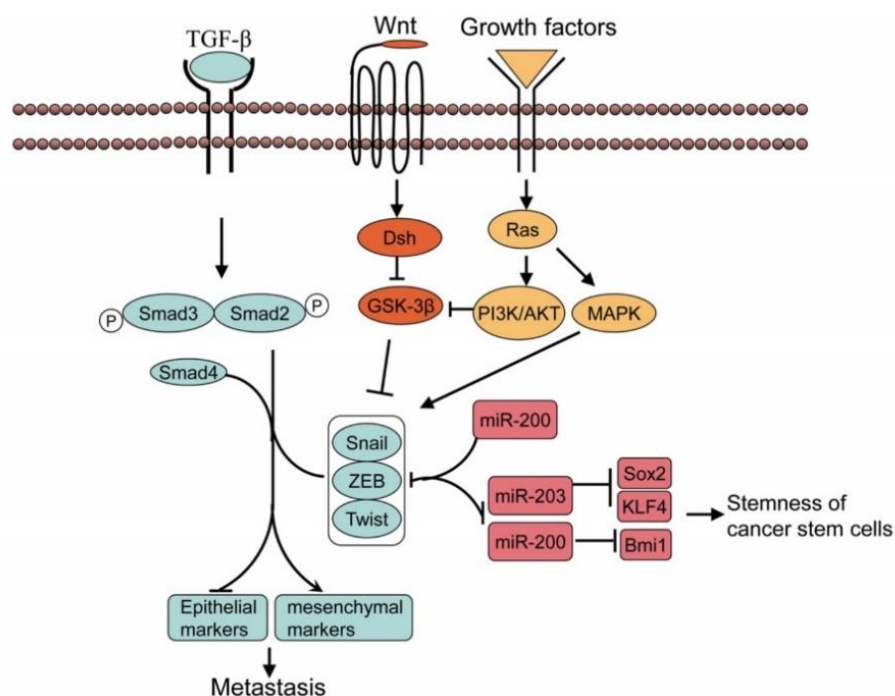


Figure 6 Schematic of the signal transduction pathways associate with EMT

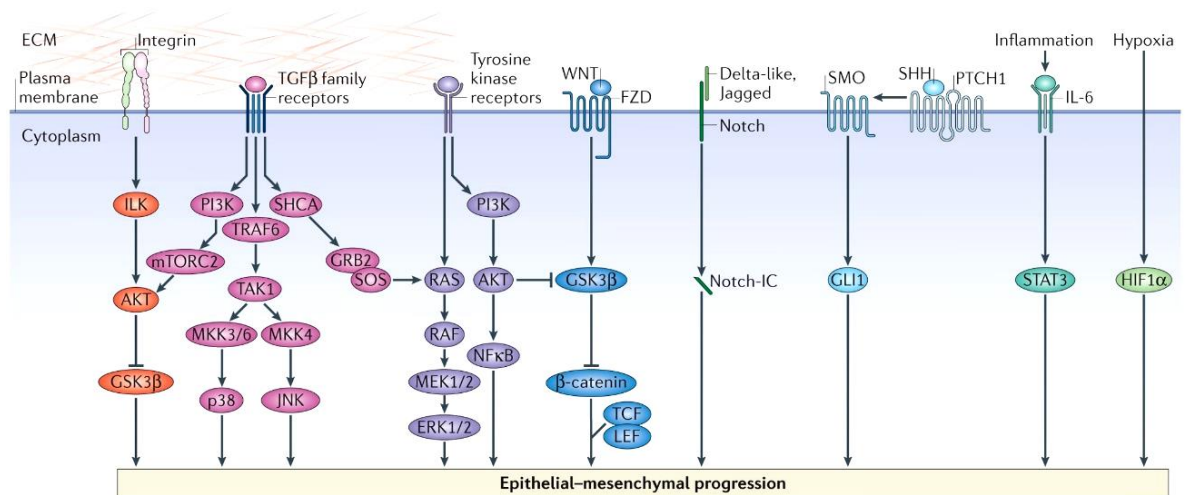
(86)

### 2.3.3 Transcriptional regulation of EMT

Loss of epithelial markers and acquisition of mesenchymal markers are common characteristics of EMT. Among these, E-cadherin depletion is a hallmark of EMT and the proliferation, intrusion and metastasis caused by loss of E-cadherin function <sup>(86)</sup>. In addition to transcription factors, Snail families (Snail and Slug), ZEB (ZEB1 and ZEB2) families, bind to consensus E-box sequences in the E-cadherin gene promoter and downregulate E-cadherin transcription <sup>(88)</sup>. Moreover, expressions of Snail and Slug were controlled via the protein degradation process. The SRD region in the central domain of snail and slug can be phosphorylated by Glycogen synthase kinase-3 $\beta$  (GSK-3 $\beta$ ) <sup>(89)</sup>. The phosphorylated Snail and Slug are ubiquitinated and degraded via proteasome <sup>(90)</sup>.

### 2.3.4 Crosstalk of signaling pathways in EMT

EMT transcription factors were shown to be induced by several mechanisms. For instance, AKT activated by integrin engagements to ECM can induce Snail expression via nuclear factor- $\kappa$ B (NF- $\kappa$ B) dependent mechanism. Moreover, active AKT was known to stabilize Snail and  $\beta$ -catenin by suppressing GSK-3 $\beta$  function <sup>(18)</sup>. Signaling pathways involved in EMT, as figure 7.



Nature Reviews | Molecular Cell Biology

Figure 7 Signaling pathways involved in EMT

(18)

### 2.3.5 Therapies targeting EMT

The goal of discovering the mechanisms governing EMT in cancer is pharmacological prevention of metastasis<sup>(88)</sup>. Especially, Inhibition of EMT could restore senescence and apoptosis capacity, which divides into 3 distinct strategies to target EMT: inhibition of extracellular EMT-inducer pathways (for example, TGF- $\beta$  blockade using rapamycin or TGF- $\beta$  receptors specific inhibitors), inhibition of EMT-transcription factors, and targeting the downstream effectors of EMT such as N-Cadherin, Vimentin, and integrins<sup>(91)</sup>.

## 2.4 Phytochemical

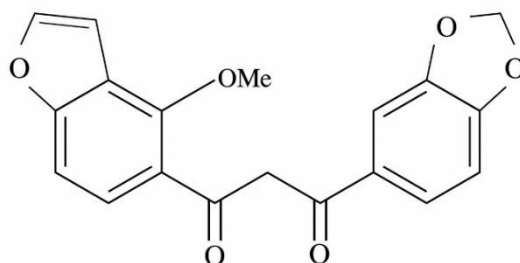


**Figure 8 Structure of ovalitenone**

Phytochemical study of *Millettia erythrocalyx* Gapnep. led to the isolation of a compounds, as show table 1<sup>(92)</sup>. Ovalitenone is a flavonoids that extracted from the roots of *M. erythrocalyx*, which chemical structure of ovalitenone is  $C_{19}H_{14}O_6$  (figure 8) and its molecular weight is 338.07904<sup>(35)</sup>. This substance can also be extracted from other species; from stem berk of *M. peguensis*<sup>(93)</sup>, as well as from seeds or roots of *Moringa ovalifolia*<sup>(94),(95)</sup>. It possesses of many effects such as anti-diabetic activity<sup>(37)</sup>, and anti-herpes simplex virus activity<sup>(38)</sup>, including uses in traditional medicine such as bleeding piles, fistulous sores, bronchitis, gonorrhea, whooping, and cough<sup>(36)</sup>.

**Table 1 Chemicals compound**

Chemicals compound	Plant part
<i>M. erythrocalyx</i>	
- Derricidin	roots
- Purpurenone	roots
- Pongaglabol	roots
- Ponganone I	roots
- Pongamol	roots
- Ovalitenone	roots
- Milletenone	roots
- Ponganone V	roots
- Lanceolatin B	roots

## CHAPTER III

### MATERIALS AND METHODS

#### 3.1 Chemicals

- 3-(4, 5-dimethylthiazol-2-yl)-2,5-diphenyltetrazolium bromide (MTT) (St. Louis, MO, USA)
- Propidium iodide (PI) (St. Louis, MO, USA)
- Hoechst 33342 (St. Louis, MO, USA)
- Triton X-100 (St. Louis, MO, USA)
- Phalloidin-rhodamine (St. Louis, MO, USA)
- Bovine serum albumin (BSA) (DA, Germany)
- Glycerol were obtained (DA, Germany)
- Fetal bovine serum (FBS) (Hercules, CA, USA)
- Agarose (Hercules, CA, USA)
- Primary antibodies from Cell Signaling Technology, Inc. (Danvers, MA)
  - N-cadherin rabbit monoclonal antibody
  - E-cadherin rabbit monoclonal antibody
  - Slug rabbit monoclonal antibody
  - Snail rabbit monoclonal antibody
  - p-mTOR rabbit monoclonal antibody
  - mTOR rabbit monoclonal antibody
  - p-FAK rabbit monoclonal antibody
  - FAK rabbit monoclonal antibody
  - p-AKT rabbit monoclonal antibody



- AKT rabbit monoclonal antibody
  - Cdc42 rabbit monoclonal antibody
  - $\beta$ -actin rabbit monoclonal antibody
- Peroxidase-conjugated secondary antibodies (Danvers, MA)
  - RIPA buffer (Danvers, MA).

### 3.2 Test compound

Ovalitenone was isolated from the roots of *Millettia erythrocalyx* Gapnep<sup>(34)</sup>. Briefly, the dried and powdered roots of this plant (8 kg) were extracted with *n*-hexane, CHCl<sub>3</sub>, and MeOH at room temperature to afford *n*-hexane extract (91 g), CHCl<sub>3</sub> extract (87 g), and MeOH extract (429 g) after removal of the solvent. The *n*-hexane extract was subjected to vacuum-liquid chromatography (VLC) on silica gel (EtOAc-pet. ether gradient) to give A-E fractions. Fraction D (36.4 g) was fractionated by VLC (silica gel, EtOAc-pet. ether gradient) and then further purified by column chromatography over silica gel (toluene), giving ovalitenone (26 mg; R<sub>f</sub> 0.24, silica gel, CHCl<sub>3</sub>-toluene 1:2). Its purity was determined using NMR spectroscopy. Ovalitenone with more than 95% purity was used in this study. Ovalitenone was dissolved in dimethyl sulfoxide (DMSO) (Sigma Chemical, St. Louis, MO, USA). The stock solution was diluted with culture medium to achieve the desired concentrations, containing less than 0.1% DMSO at final concentrations.

### 3.3 Cell culture

Human NSCLC H460 and A549 cells were obtained from the American Type Culture Collection (Manassas, VA, USA). H460 and A549 cells were cultured in Roswell Park Memorial Institute (RPMI) 1640 medium (Gibco, Grand Island, NY, USA) and Dulbecco's Modified Eagle's Medium (DMEM) (Gibco, Grand Island, NY, USA),

respectively. The culture media were supplemented with 10% fetal bovine serum (FBS) (Merck, DA, Germany), 2 mM L-glutamine (Gibco, Grand Island, NY, USA) and 100 U/ml penicillin and streptomycin (Gibco, Grand Island, NY, USA), and incubated at 37 °C with 5% CO<sub>2</sub> in a humidified incubator.

### 3.4 Methods

#### 3.4.1 Cell viability and cell proliferation assay

Cell viability and cell proliferation were examined by MTT assay. Cells (1×10<sup>4</sup> cells/well for cell viability and 2×10<sup>3</sup> cells/well for cell proliferation) were seeded onto each well of a 96-well plates and incubated overnight for cell attachment. Cells were treated with various concentrations of ovalitenone (0-200 μM) for 24 h for the cell viability assay and were extended time to 48 and 72 h for cell proliferation assay. After treatments, the culture media were removed and incubated with 400 μg/ml of MTT at 37 °C for 3 h and the formazan crystals were solubilized in 100 μl DMSO and measured at wavelength 570 nm with microplate reader (Anthros, Durham, NC, USA). The percentage of cell viability was calculated as absorbance of ovalitenone treated cells relative to the untreated cells. The proliferation rates were determined using the following equation:

$$\text{Cell viability (\%)} = \frac{\text{Absorbance of treated cells}}{\text{Absorbance of controlled cells}} \times 100$$

#### 3.4.2 Nuclear staining assay

H460 and A549 cells were seeded onto 96-well plates at a density of 1×10<sup>4</sup> cells/well and incubated at 37 °C with 5% CO<sub>2</sub> for overnight. Cells were treated with ovalitenone at various concentration (0-200 μM) and incubated at 37 °C with 5% CO<sub>2</sub> for 24 h. After treatments, cells were co-stained with 10 μM of Hoechst 33342 (Sigma, St. Louis, MO, USA) and propidium iodide (PI) (Sigma, St. Louis, MO, USA) for 15 min at

37 °C. Cells were visualized and imaged using a fluorescence microscopy (Olympus DP70, Melville, NY, USA). Three random fields were captured at 20x magnification and then the percentages of apoptotic cells were calculated.

$$\text{Apoptotic cells (\%)} = \frac{\text{Number of apoptotic cells}}{\text{Number of live cells}} \times 100$$

$$\text{Necrotic cells (\%)} = \frac{\text{Number of necrotic cells}}{\text{Number of live cells}} \times 100$$

### 3.4.3 Apoptosis assay

Apoptotic and necrotic were evaluated using Annexin V-FITC apoptosis Kit (Thermo Fisher Scientific, Waltham, MA, USA). H460 and A549 cells were seeded onto 6-well plates at a density of  $2.5 \times 10^4$  cells/well and incubated at 37 °C for overnight. Cells were treated with ovalitenone at concentrations 100 and 200  $\mu\text{M}$ , and incubated at 37 °C for 24, 48 and 72 h. After that, cells were detached with trypsin-EDTA (0.25%), washed with PBS, and centrifuged at 1500 rpm for 5 min. Cells were suspended with 1x binding buffer and incubated into Annexin and PI at room temperature for 15 min in the dark. Apoptotic and necrotic cells were analyzed using guava easyCyte™ flow cytometry (Merk, DA, Germany).

### 3.4.4 Colony formation assay

H460 and A549 cells were seeded onto 6-well plates at a density 300 cells/well and incubated at 37 °C for overnight. The culture medium was replaced with fresh medium containing ovalitenone at non-toxic concentrations (0-200  $\mu\text{M}$ ), and the cells were incubated for 7 days. The cells were washed twice with 1x PBS, fixed with 4% paraformaldehyde (Sigma Chemical, St. Louis, MO, USA) for 20 min, and 30 min-staining with Crystal violet solution at room temperature. After washing with tap water, the colonies were counted and the results were representative of three independents.

$$\text{Colony number (\%)} = \frac{\text{Number of treated cells}}{\text{Number of untreated cells}} \times 100$$

### 3.4.5 Migration assay

Migration was determined by wound healing assay. H460 and A549 cells were cultured as monolayer in 96-well plates. The bottom of each well was scratched using sterile 1-mm-wide pipette tip (P200 micropipette tip). Culture medium was removed and washed by 1x PBS. The monolayer cells were incubated with ovalitenone at non-toxic concentrations (0-200  $\mu\text{M}$ ) at 37  $^{\circ}\text{C}$  for 24, 48 and 72 h, respectively. At indicated time points, migration was observed under a phase contrast microscope (Olympus, Melville, NY, USA) and images were captured using Olympus DP70 digital camera with Olympus DP controller software (Olympus). The wound area was determined by ImageJ software, and the percentage of wound closure was calculated as an equation following:

$$\text{Wound closure (\%)} = \left[ \frac{(A_0 - A_{\Delta h})}{A_0} \right] \times 100$$

where,  $A_0$  is the area of the wound measured immediately after scratching (0 h), and  $A_{\Delta h}$  is the area of the wound measured at 24, 48 or 72 h after treatment. Relative cell migration was calculated by dividing the percentage change in the wound space of treated cells by that of the control cells in each experiment.

### 3.4.6 Cell morphology and filopodia characterization

Cell morphology and filopodia was investigated by a phalloidin-rhodamine staining assay. The cells were seeded in 96-well plates for overnight. Cells were treated with ovalitenone at non-toxic concentration (0-200  $\mu\text{M}$ ) for 24 h. After treatments, the treated cells were washed with 1x PBS and fixed with 4% paraformaldehyde (Sigma Chemical, St. Louis, MO, USA) in 1x PBS for 10 min at 37  $^{\circ}\text{C}$ . Then, cells were

permeabilized with 0.1% Triton X-100 (Sigma Chemical, St. Louis, MO, USA) in 1x PBS for 4 min and blocked with 0.2% bovine serum albumin (BSA) (Merck, DA, Germany) for 30 min. Subsequently, cells were incubated with a phalloidin-rhodamine (Sigma Chemical, St. Louis, MO, USA) in 1x PBS for 15 min, and mounted with 50% glycerol (Merck, DA, Germany). Cell morphology and filopodia were assessed under fluorescence microscope (Nikon ECLIPSE Ts2, Tokyo, Japan). Relative number of filopodia/cell was determined the number of filopodia/cell of the ovalitenone-treated cells dividing by control cells.

#### **3.4.7 Invasion assay**

Cell invasion was performed by using transwell Boyden chamber (8  $\mu\text{m}$  pore size; BD Bioscience, MA, USA). H460 and A549 cells were treated with ovalitenone at non-toxic concentrations (0-200  $\mu\text{M}$ ) for 24 h before subjecting to invasion evaluation. The upper chamber was coated with 0.5% Matrigel (BD Biosciences, San Jose, CA, USA) overnight at 37 °C. Then, the treated cells were seeded at a density of  $2 \times 10^4$  cells/well in the upper chamber supplemented with serum free medium, while the complete medium containing 10% FBS (Merck, DA, Germany) were added to the lower chamber compartment as a chemoattractant. After incubation at 37 °C for 24 h, the non-invading cells in the upper chamber were removed with a cotton swab and the invading cells in the lower chamber were fixed with cold methanol (Merck, DA, Germany) for 10 minutes and stained with 10  $\mu\text{M}$  of Hoechst 33342 (Sigma, St. Louis, MO, USA) for 10 minutes. Finally, the stained cells were visualized and captured using a fluorescence microscope (Nikon ECLIPSE Ts2, Tokyo, Japan). Relative invasion was calculated by dividing the number of invaded cells treated with ovalitenone compared to the non-treated cells in each experiment.

#### 3.4.8 Anchorage-independent growth assay

Anchorage-independent growth was determined by the soft agar colony-formation assay. Briefly, H460 and A549 cells were pre-treated with ovalitenone at non-toxic concentrations (0-200  $\mu\text{M}$ ) for 24 h at 37 °C. The bottom layer was prepared by using a 1:1 mixture of RPMI-1640 or DMEM medium containing 10% FBS (Merck, DA, Germany) and 1% agarose, then were allowed to solidify for 20 min at 4 °C. The upper layer consisting of 0.3% agarose gel with 10% FBS (Merck, DA, Germany) and containing  $1 \times 10^3$  cells/ml were prepared and added. RPMI-1640 or DMEM medium containing 10% FBS (Merck, DA, Germany) was added over upper layer. Cells were incubated for 14 days at 37 °C and colony formation were counted and captured using a phase-contrast microscope (Nikon ECLIPSE Ts2, Tokyo, Japan). Relative colony number and size was counted and calculated by dividing the values of the treated cells by the non-treated cells.

#### 3.4.9 Spheroid formation assay

H460 and A549 cells were pre-treated with non-toxic concentrations of ovalitenone (0-200  $\mu\text{M}$ ) for 24 h at environment 37 °C with 5%  $\text{CO}_2$ . The treated cells were seeded at a density of  $2.5 \times 10^3$  cells/well onto an ultralow-attachment plate in culture medium containing 1% (v/v) FBS (Merck, DA, Germany) for 14 days to form primary spheroids. The primary spheroids were suspended into single cells, and then these cells were grown in a 24-well ultralow-attachment plate at a density of  $2.5 \times 10^3$  cells/well for 21 days to form secondary spheroids. At days 7, 14, and 21, the numbers and sizes of secondary spheroids were determined and imaged using a phase-contrast microscopy (Nikon ECLIPSE Ts2, Tokyo, Japan).

#### 3.4.10 Western blot Analysis

After ovalitenone at non-toxic concentrations (0-200  $\mu\text{M}$ ) treatment, cells were incubated on ice for 40 min with RIPA buffer, 1% Triton X-100, 100 mM PMSF, and a protease inhibitor. Cell lysates were analyzed for protein content using the BCA protein assay kit from Pierce Biotechnology (Rockford, IL). Equal amounts of protein samples (Approximately 60-100  $\mu\text{g}$ ) were separated by sodium dodecyl sulfate polyacrylamide gel electrophoresis (SDS-PAGE) and transferred to polyvinylidene difluoride (PVDF) (Bio-Rad Laboratories Inc., CA, USA) or nitrocellulose membranes (Bio-Rad Laboratories Inc., CA, USA). The resulting blots were blocked for 2 h with 5% (w/v) non-fat dry milk (Merck, DA, Germany) in TBS-T (Tris-buffer saline with 0.1% Tween containing 25 mM Tris-HCl (pH 7.5), 125 mM NaCl, and 0.1% Tween 20) and incubated with the specific primary antibodies against N-cadherin, E-cadherin, Snail, Slug, p-mTOR, mTOR, p-FAK, FAK, p-AKT, AKT, Cdc42, and  $\beta$ -actin (Cell Signaling, Danvers, MA, USA) at 4 °C overnight. After three washed with TBS-T, the membranes were incubated with horseradish peroxidase (HRP)-conjugated secondary antibodies (Cell Signaling, Danvers, MA, USA) for 2 h at room temperature. Finally, the immune blots were detected by enhanced chemiluminescence (Supersignal West Pico; Pierce, Rockford, IL, USA) and quantified using ImageJ software (NIH, Bethesda, MD, USA).

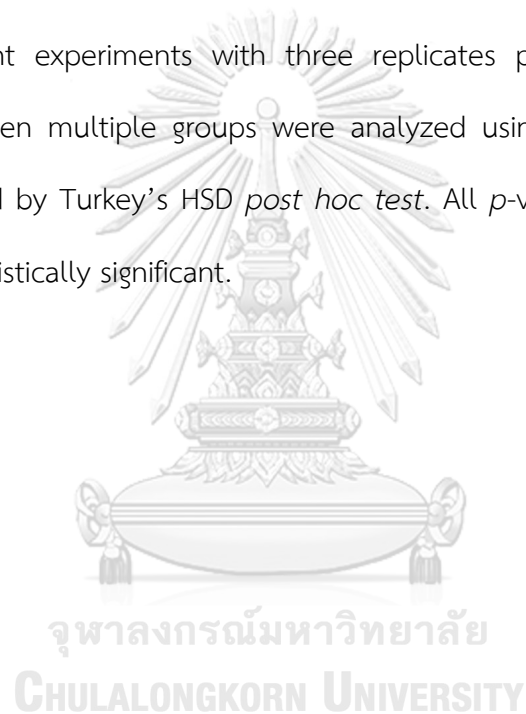
#### 3.4.11 Immunofluorescence assay

Cells were seeded onto 96-well plates at a density  $1 \times 10^4$  cells/well and incubated overnight. The cells were treated with ovalitenone for 24 h. The cells were washed twice with 1x PBS and fixed with 4% paraformaldehyde for 20 min, permeabilized with 0.1% Triton-x in PBS for 20 min, and blocked with 4% BSA in 1x PBS for 30 min at room temperature. The cells were incubated with primary antibodies at 4 °C overnight, the cells were washed twice with 1x PBS and incubated with

secondary antibody for 1 h in the dark at room temperature. The cells were washed with 1x PBS and incubated with Hoechst 33342 (Sigma, St. Louis, MO, USA) for 20 min in the dark, rinsed with 1x PBS and mounted by 50% glycerol (Merck, DA, Germany). Imaging was assessed under fluorescence microscope with a 40x objective lens (Nikon ECLIPSE Ts2, Tokyo, Japan).

### 3.5 Statistical analysis

The data was presented as the mean  $\pm$  standard error of the mean (SEM) of three independent experiments with three replicates per experiment. Statistical differences between multiple groups were analyzed using an analysis of variance (ANOVA), followed by Turkey's HSD *post hoc test*. All *p*-values less than 0.05 were considered as statistically significant.





## CHAPTER IV

## RESULTS

## 4.1 Effect of ovalitenone on cell viability and proliferation of H460 and A549 cells

Ovalitenone, isolated from *Millettia erythrocalyx*, was used in this study. To determine the non-toxic concentrations of ovalitenone to be used in the following experiments, human NSCLC H460 and A549 cells were treated with various concentrations of ovalitenone (0–200  $\mu\text{M}$ ) for 24 h, and cell viability was measured by 3-(4,5-dimethylthiazol-2-yl)-2,5 diphenyltetrazolium bromide (MTT) assay. The results revealed that ovalitenone at concentrations lower than 200  $\mu\text{M}$  did not significantly affect the viability in both cells (Figure 9).

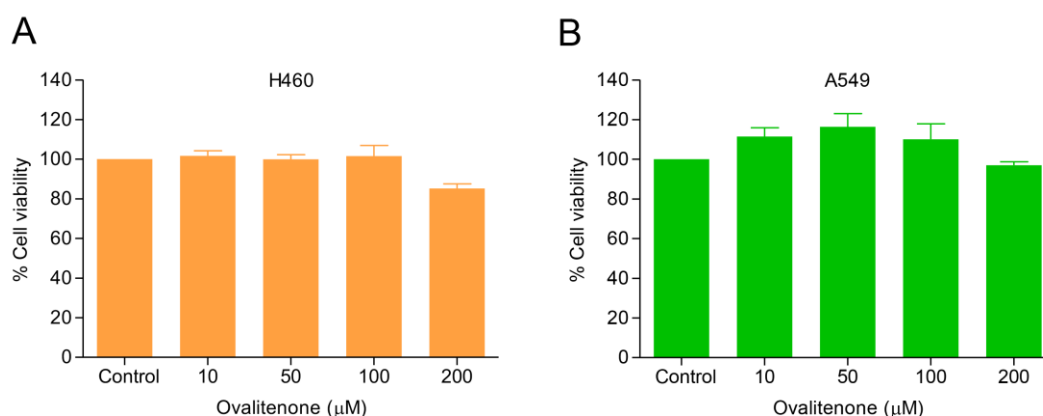


**Figure 9** Effect of ovalitenone on cell viability of H460 and A549 cells.

(A-B) Cell viability of the cells was assessed by MTT assay. All data are presented as mean  $\pm$  SEM ( $n = 3$ ). \* $p < 0.05$  compared with untreated cells.

For cell proliferation analysis, H460 and A549 cells were treated with various concentrations of ovalitenone (0–200  $\mu\text{M}$ ) for 24, 48, and 72 h, and their viability was evaluated. The results shown that ovalitenone at concentrations of 0–200  $\mu\text{M}$  had no effect on cell proliferation in H460 and A549 cells at 24 h (Figure 10); however, the rate of proliferation of the treated cells was significantly decreased in a dose-dependent manner at concentrations of 50 to 200  $\mu\text{M}$  at 48 h, while ovalitenone at concentrations of 10 to 200  $\mu\text{M}$  significantly decreased proliferation at 72 h in both cells (Figure 10).

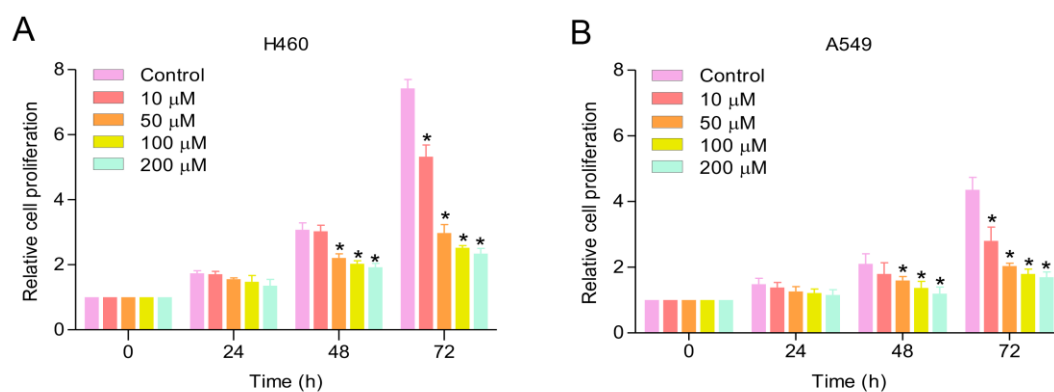


**Figure 10** Effect of ovalitenone on cell proliferation of H460 and A549 cells.

(A-B) Effect of ovalitenone on cell proliferation was performed by MTT assay. All data are presented as mean  $\pm$  SEM ( $n = 3$ ). \* $p < 0.05$  compared with untreated cells.

In order to investigate the apoptosis induction of ovalitenone in H460 and A549 cells, nuclear staining assay was performed. Cells were treated with ovalitenone at 0–200  $\mu\text{M}$  for 24, 48 and 72 h, and treated cells were stained with Hoechst 33342 and propidium iodide (PI). The results indicated that ovalitenone at 0–200  $\mu\text{M}$  had no effect on apoptosis or necrosis in H460 and A549 cells (Figure 11).

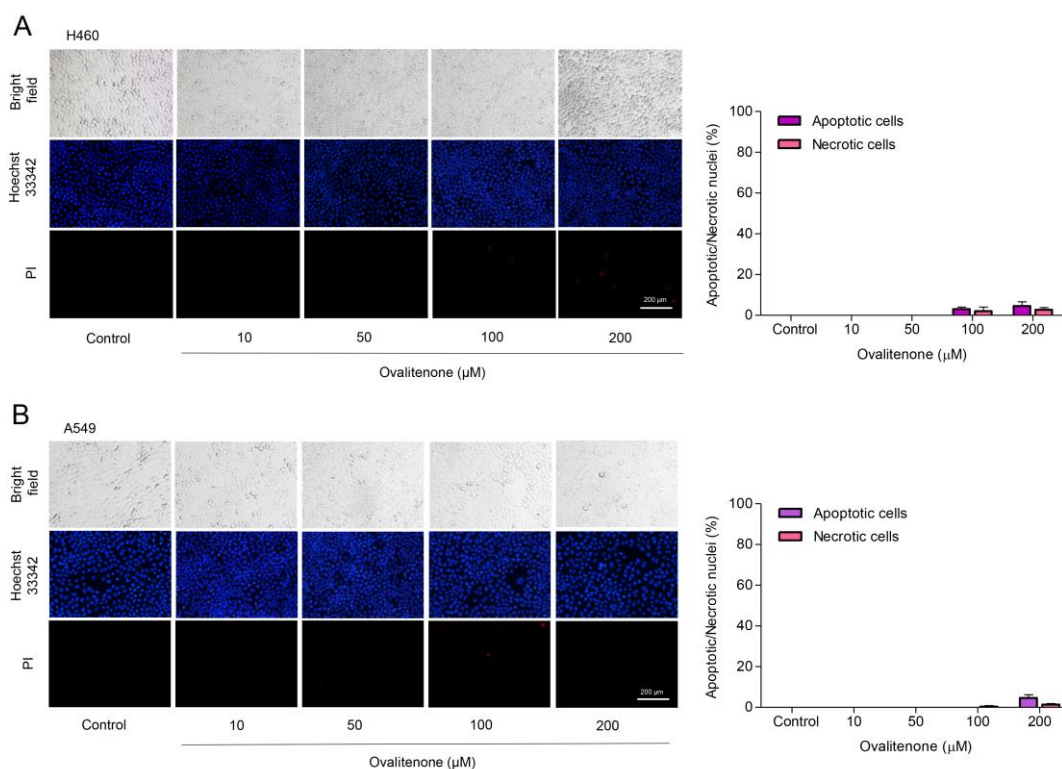


**Figure 11 Apoptosis effect of ovalitenone on H460 and A549 cells.**

(A-B) The cells were treated with ovalitenone for 24 h, and apoptotic and necrotic cells were evaluated by Hoechst 33342 and PI staining. All data are presented as mean  $\pm$  SEM (n = 3). \* $p$  < 0.05 compared with untreated cells.

To confirm, apoptosis and necrosis cells in response to ovalitenone treatment were determined by annexin V/PI assay. Flowcytometry analysis revealed that ovalitenone at the concentrations of 100 and 200  $\mu\text{M}$  did not cause either apoptosis or necrosis in both cells at 24, 48, and 72 h (Figure 12-13).

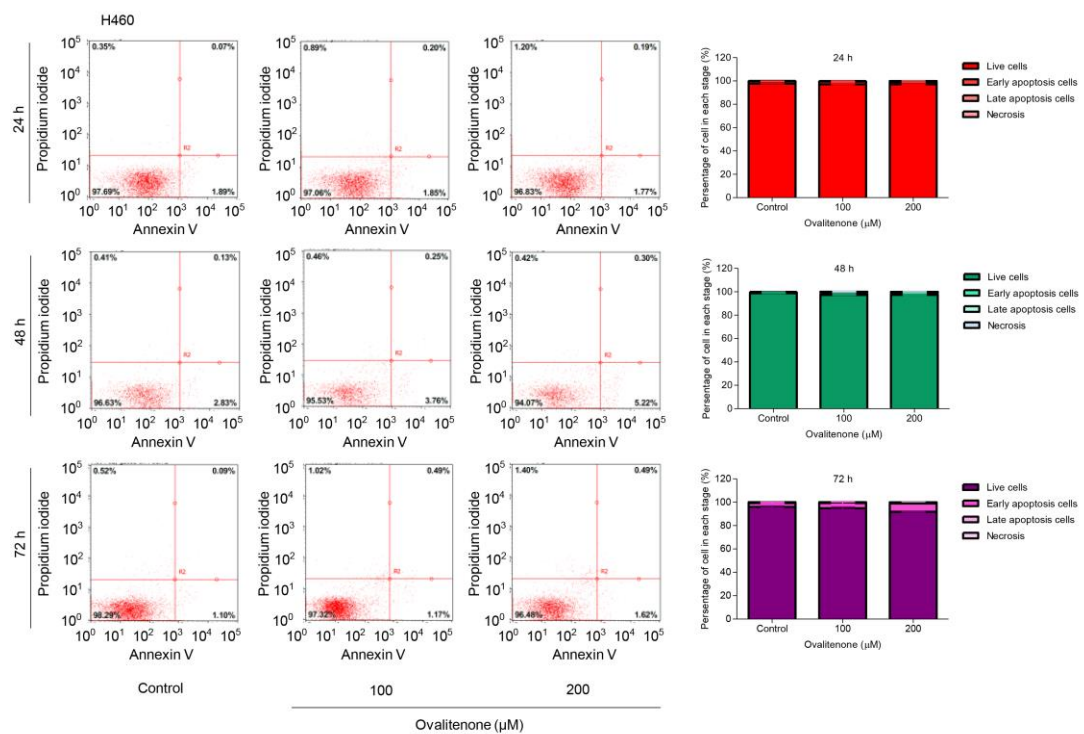


**Figure 12 Effect of ovalitenone on apoptosis by flow cytometry in H460 cells.**

Annexin V/PI co-stained cells were examined using flow cytometry. All data are presented as mean  $\pm$  SEM ( $n = 3$ ).  $*p < 0.05$  compared with untreated cells.

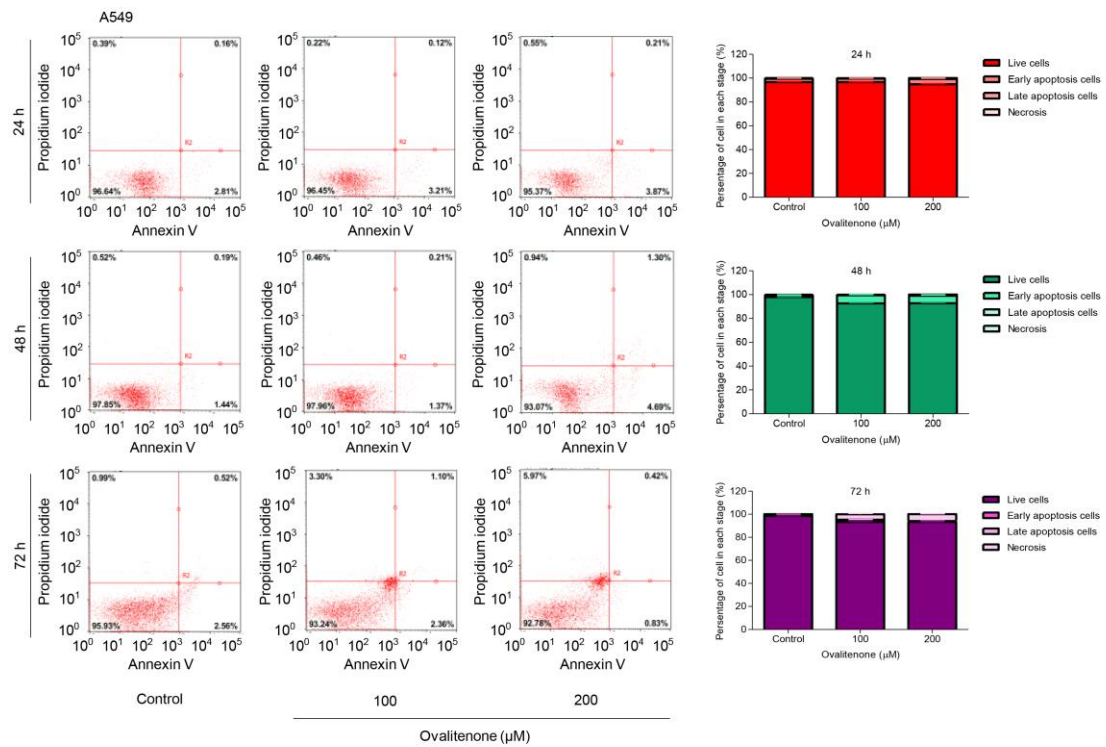
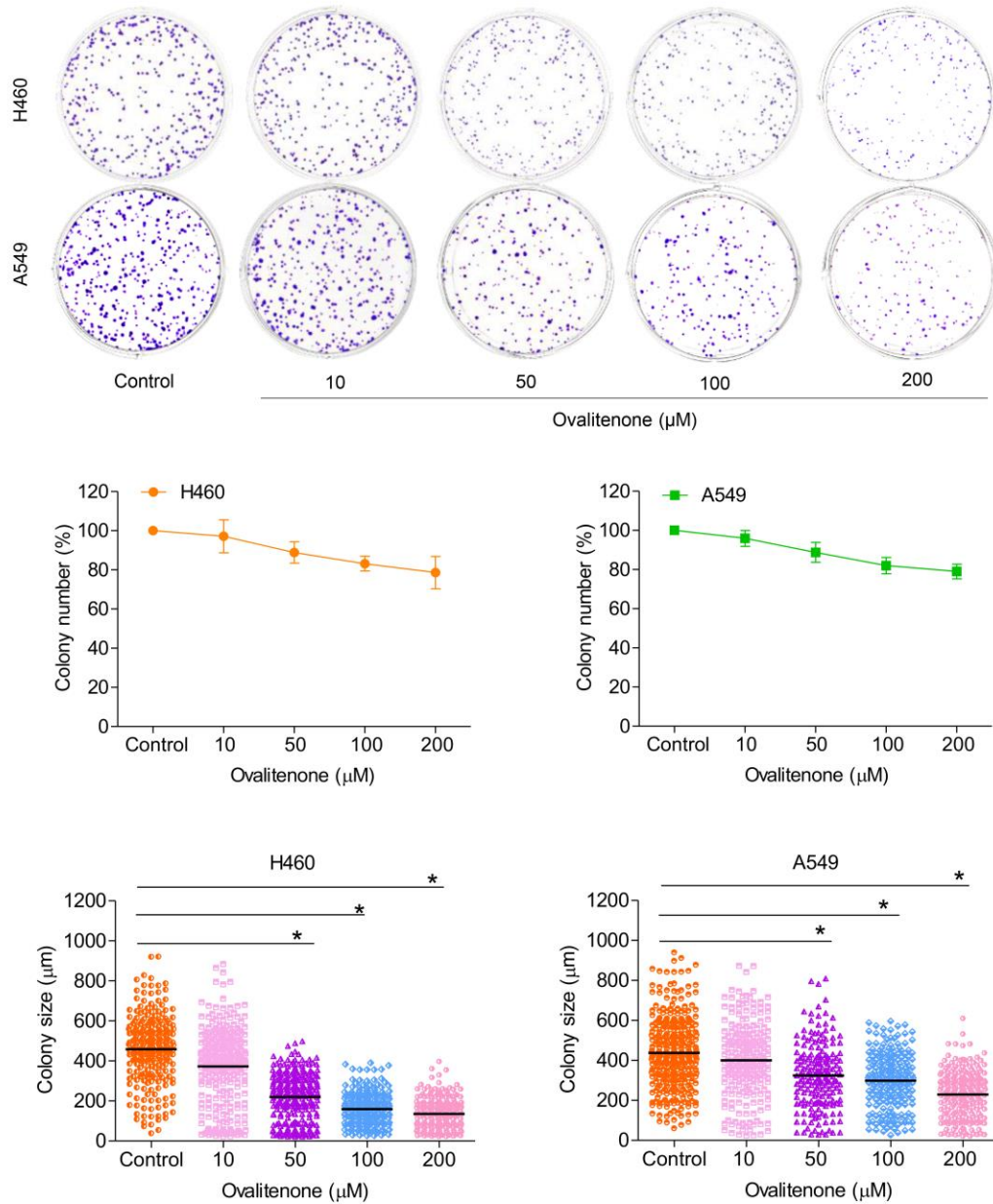


Figure 13 Effect of ovalitenone on apoptosis by flow cytometry of A549 cells.

Annexin V/PI co-stained cells were examined using flow cytometry. All data are presented as mean  $\pm$  SEM ( $n = 3$ ). \* $p < 0.05$  compared with untreated cells.

Confirmation the effect of ovalitenone on cell proliferation by colony formation assay, and the results shown that ovalitenone at 50 to 200  $\mu\text{M}$  could decrease the size of the colonies in H460 and A549 cells (Figure 14). Here, non-toxic concentrations of ovalitenone were used for the further anti-migration and invasion experiments described below.



**Figure 14** Effect of ovalitenone on cell proliferation by colony formation assay in H460 and A549 cells.

Cells were treated as indicated for 7 days, and colony was stained by crystal violet. All data are presented as mean  $\pm$  SEM ( $n = 3$ ). \* $p < 0.05$  compared with untreated cells.

#### 4.2 Effect of ovalitenone on lung cancer cell migration, invasion and filopodia formation

Investigating the effect of ovalitenone on the migration and invasion properties of lung cancer cells. Cell migration was determined by a wound-healing assay, whereby wounded monolayers of H460 and A549 cells were treated with ovalitenone at non-toxic concentrations (0–200  $\mu\text{M}$ ) for 24, 48, and 72 h, respectively. The results revealed that ovalitenone inhibited H460 and A549 cells migration at concentrations of 50 to 200  $\mu\text{M}$  at 24, 48, and 72 h, whereas ovalitenone at 10  $\mu\text{M}$  did not significantly inhibit the cells migration (Figure 15). Additionally, cell invasion was determined using a transwell Boyden chamber coated with Matrigel. Cells were seeded on the Matrigel surface in the presence or absence of ovalitenone (0–200  $\mu\text{M}$ ), and the invaded cells at other sites of the membrane were counted at 24 h. Figure 16 shown that the ovalitenone was able to inhibit cell invasion through the Matrigel layer. Cell protrusion facilitating cell migration was further evaluated in the cells treated with non-toxic concentrations of ovalitenone. Analysis by phalloidin staining indicated that ovalitenone treatments significantly reduced the number of filopodia per cells (Figure 17). Taken together, our results reveal the anti-migratory activities of ovalitenone.

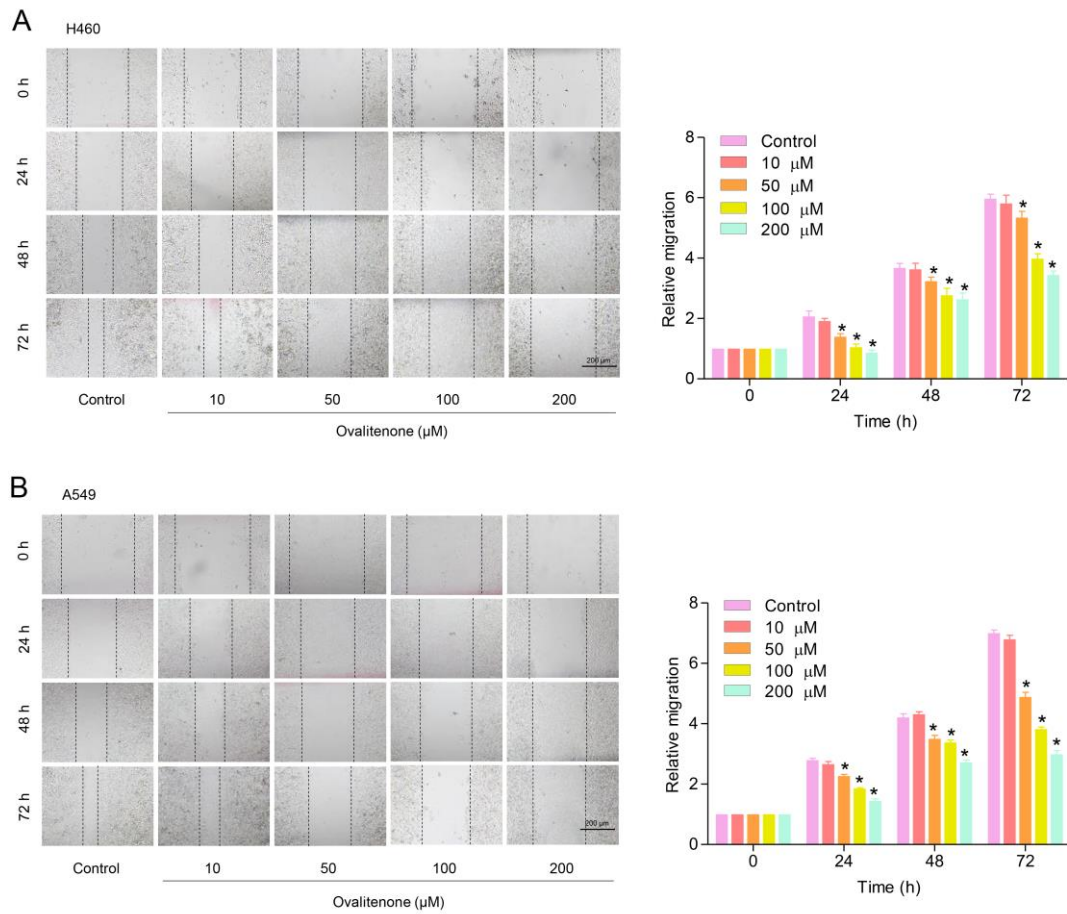


**Figure 15** Ovalitenone suppressed cell migration in H460 and A549 cells.

(A-B) Cells were treated with ovalitenone for 24, 48, and 72 h, and migration activity was determined by wound healing assay. All data are represented as mean  $\pm$  SEM (n = 3). \* $p$  < 0.05 compared with untreated cells.



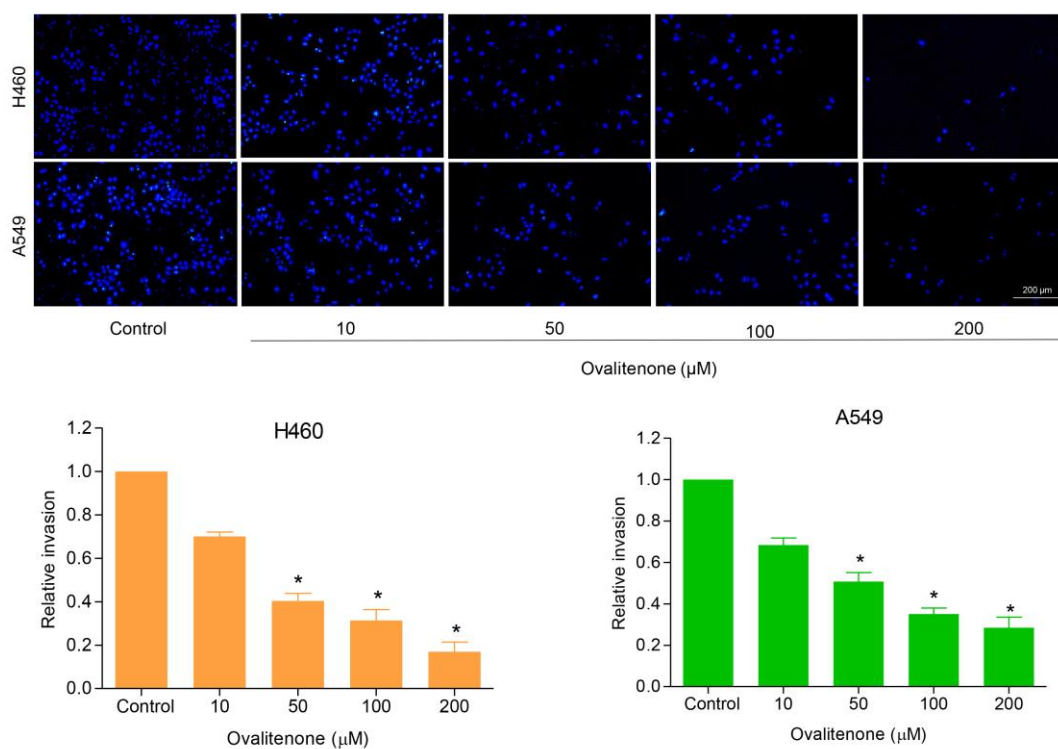


**Figure 16** Ovalitenone suppressed cell invasion in H460 and A549 cells.

Cell invasion was examined by transwell invasion assay. After 24 h, invading cells were stained with Hoechst 33342 and photographed. All data are represented as mean  $\pm$  SEM (n = 3). \* $p$  < 0.05 compared with untreated cells.

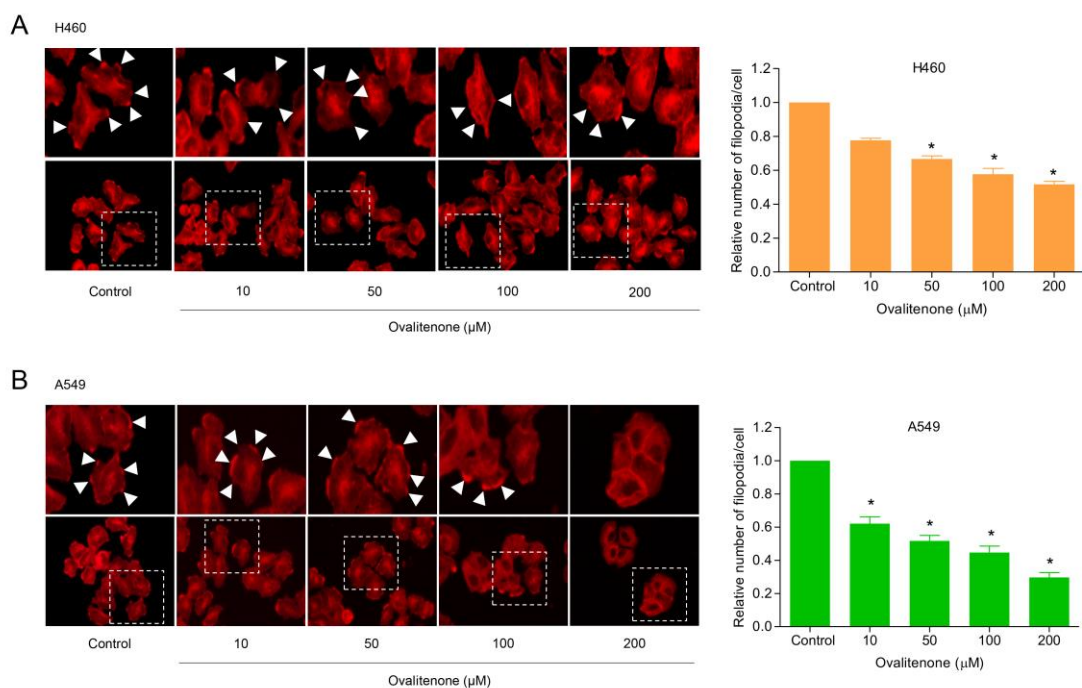


**Figure 17** Ovalitenone suppressed filopodia formation in H460 and A549 cells. (A-B) Cells were treated with ovalitenone for 24 h, filopodia was stained with phalloidin-rhodamine, and the number of filopodia per cells was counted. All data are represented as mean  $\pm$  SEM ( $n = 3$ ). \* $p < 0.05$  compared with untreated cells.

### 4.3. Ovalitenone attenuates anchorage-independent growth and CSC-like phenotypes of human lung cancer H460 and A549 cells

It was previously reported that the process of the anchorage-independent growth of cancer cells reflects anoikis resistance and the metastasis potential of malignant tumor cells<sup>(96)</sup>. To test whether ovalitenone could suppress such cancer cell growth under attached conditions, H460 and A549 cells were grown in soft agar in the presence or absence of ovalitenone for 14 days. The number and size of the growing cancer colonies were determined and calculated relative to those with the untreated control. The results indicated that the ovalitenone-treated cells (at concentrations of 50 to 200  $\mu\text{M}$ ) significantly reduced ability to form colonies, and treatment with the compound could attenuate the growth of the cells as indicated by the decrease in colony number and size when compared with the untreated control in both cells (Figure 18). As illustrated in Figure 18 A, the colony numbers of H460 cells were significantly reduced by ovalitenone treatment at 50, 100, and 200  $\mu\text{M}$  to 31.05%, 51.48%, and 73.20%, respectively, and the percentages of colony size in response to ovalitenone at the concentrations of 50, 100, and 200  $\mu\text{M}$  were 33.82%, 50.61%, and 63.41%, respectively. The colony numbers of A549 (Figure 18 B) cells were significantly reduced by ovalitenone at 50, 100, and 200  $\mu\text{M}$  to 38.93%, 50.37%, and 74.06%, respectively, and the percentages of colony size in response to the compound at 50, 100, and 200  $\mu\text{M}$  were 31.62%, 49.92%, and 66.36%, respectively. These results suggest that ovalitenone at non-toxic doses could inhibit the survival and growth of human lung cancer cells under detached conditions.

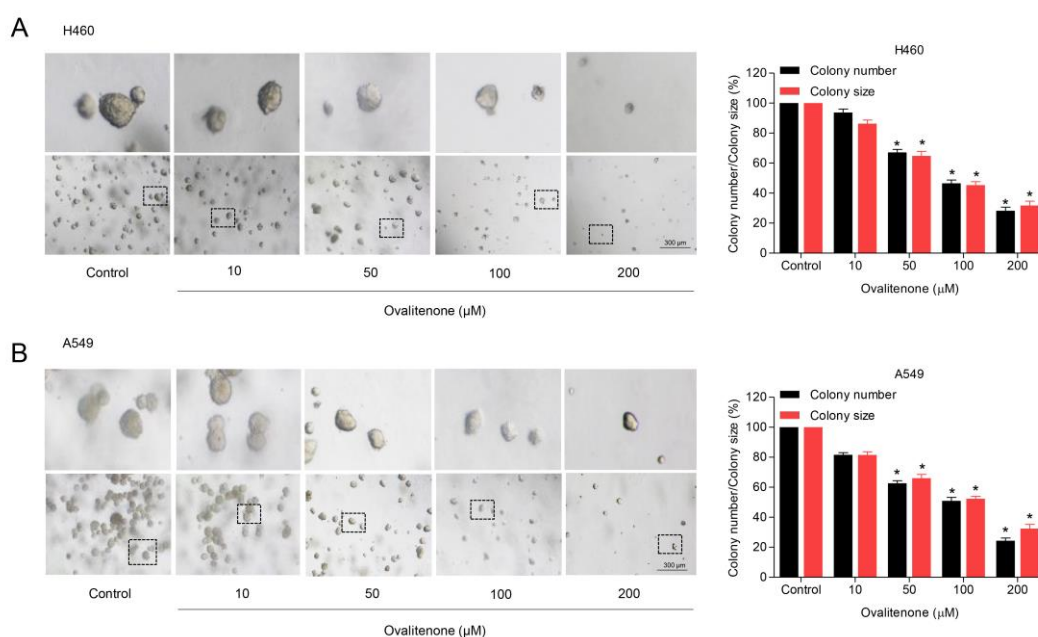


**Figure 18 Ovalitenone attenuates anchorage-independent growth of H460 and A549 cells.**

(A-B) Cells were pre-treated with sub-toxic concentrations of ovalitenone for 24 h, and were subjected to an anchorage-independent growth assay. All data are represented as mean  $\pm$  SEM ( $n = 3$ ). \* $p < 0.05$  compared with untreated cells.

As the ability of cancer cells to form spheroids has been used to reflect CSC phenotypes and as CSCs are well known to have a very high metastatic potential, next study evaluated the effect of ovalitenone on CSCs. H460 and A549 cells were treated with non-toxic concentrations of ovalitenone (0–200  $\mu\text{M}$ ) for 24 h, and the cells were subjected to a spheroid formation assay. After secondary spheroids were formed, the results shown that the non-treated control cells had a highly ability to form tumor spheroids, whereas cells treated with ovalitenone reduced presence of tumor spheroids in a dose-dependent manner (Figure 19-20). Ovalitenone at concentrations from 50 to 200  $\mu\text{M}$  significantly decreased the number and size of the primary and secondary spheroids compared with the control in both H460 and A549 cells (Figure 19-20). Taken together, ovalitenone possessed anti-metastasis activities as it could

suppress cancer migration, invasion, and growth under anchorage-independent conditions and could also suppress the CSC-like phenotypes.

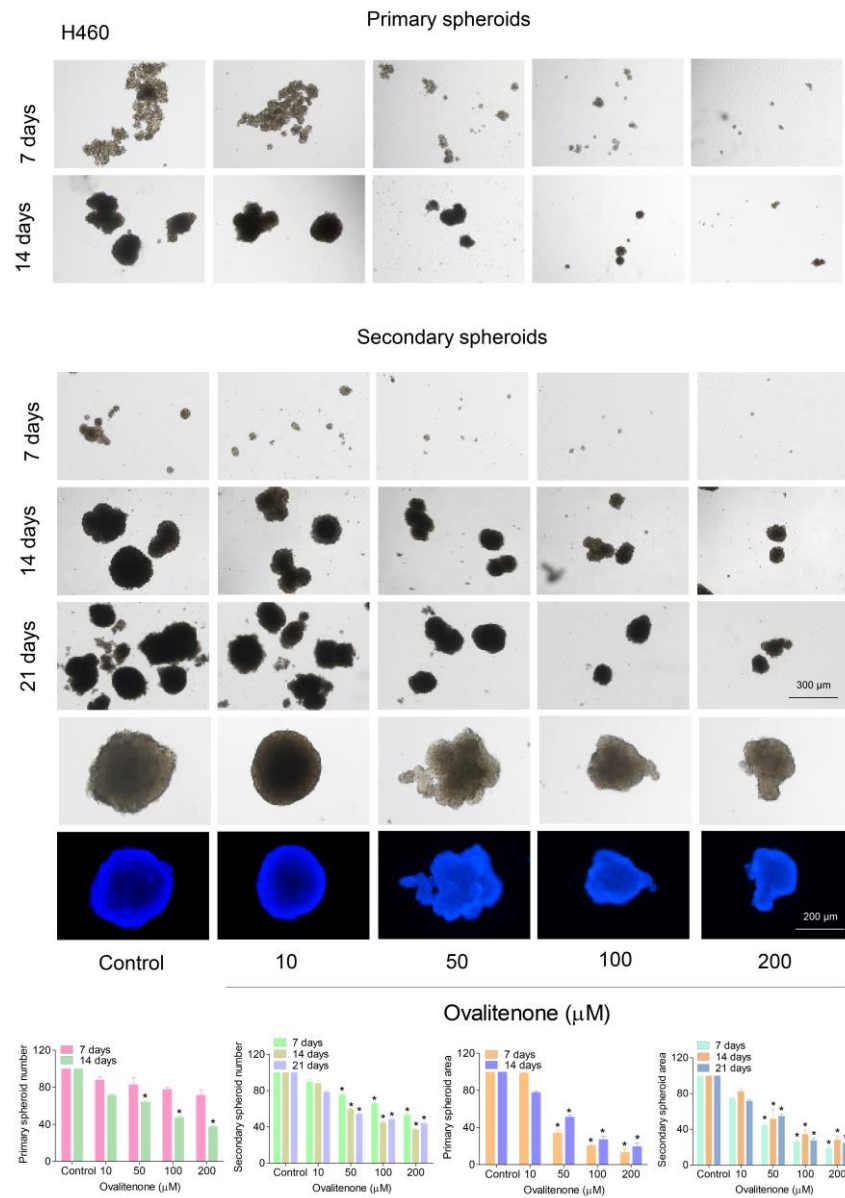


**Figure 19** Ovalitenone attenuates cancer stem cell (CSC)-like phenotypes of H460 cells.

Cells were pre-treated with non-toxic concentrations of ovalitenone for 24 h, and allowed for 14 days to form primary spheroids. After, the primary spheroids were suspended into single cells to form secondary spheroids for 21 days, the spheroid of cancer stem cell (CSC)-rich population was determined. All data are represented as mean  $\pm$  SEM ( $n = 3$ ).  $*p < 0.05$  compared with untreated cells.

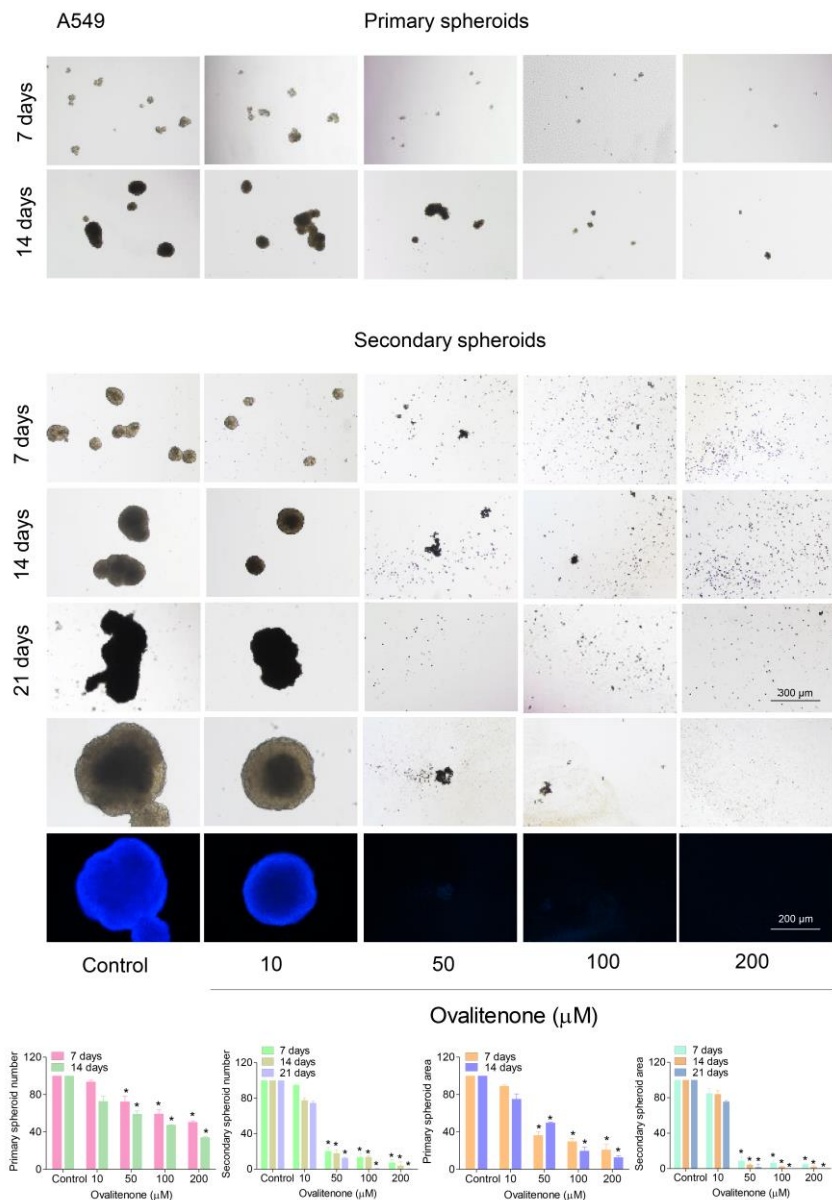
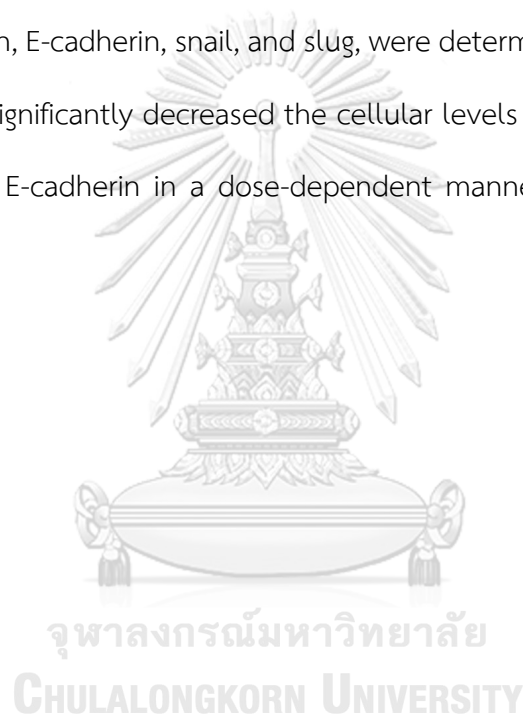


**Figure 20 Ovalitenone attenuates cancer stem cell (CSC)-like phenotypes of A549 cells.**

Cells were pre-treated with non-toxic concentrations of ovalitenone for 24 h, and allowed for 14 days to form primary spheroids. After, the primary spheroids were suspended into single cells to form secondary spheroids for 21 days, the spheroid of cancer stem cell (CSC)-rich population was determined. All data are represented as mean  $\pm$  SEM ( $n = 3$ ). \* $p < 0.05$  compared with untreated cells.

#### 4.4. Ovalitenone suppresses EMT via the suppression of the AKT/mTOR signalling pathway

EMT has been well linked with metastasis and is known to be a cellular process that can facilitate migration and invasion, anoikis resistance, and the CSCs of cancer cells <sup>(12)</sup>. Evaluating the underlying mechanism of ovalitenone action. Firstly, determines the EMT makers in cells exposed to ovalitenone. Cells were treated with ovalitenone (0–200  $\mu$ M) for 24 h, and the levels of the well-recognized EMT markers, namely, N-cadherin, E-cadherin, snail, and slug, were determined. The results indicated that ovalitenone significantly decreased the cellular levels of N-cadherin and snail, as well as increased E-cadherin in a dose-dependent manner in H460 and A549 cells (Figure 21-22).



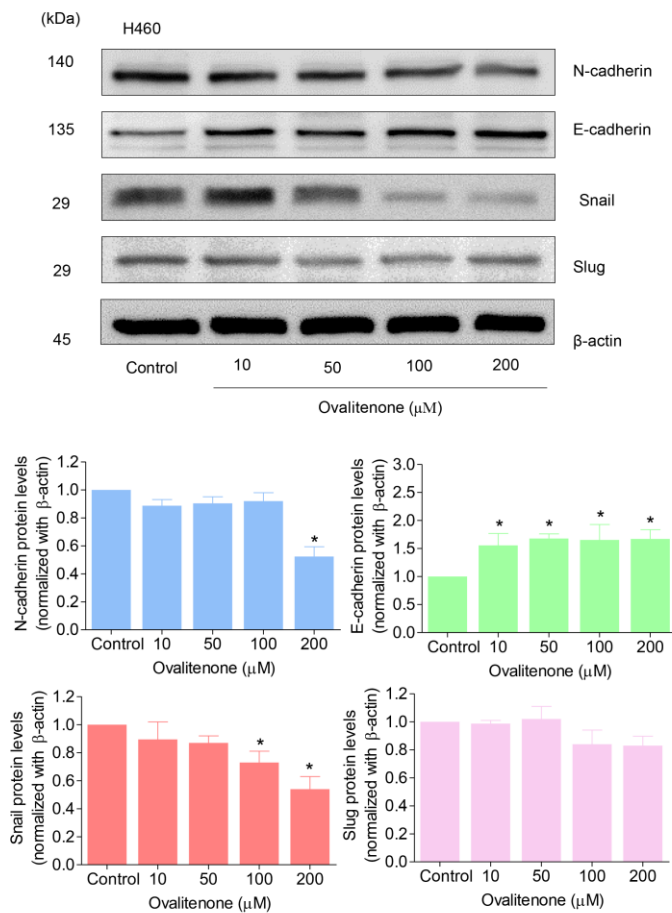
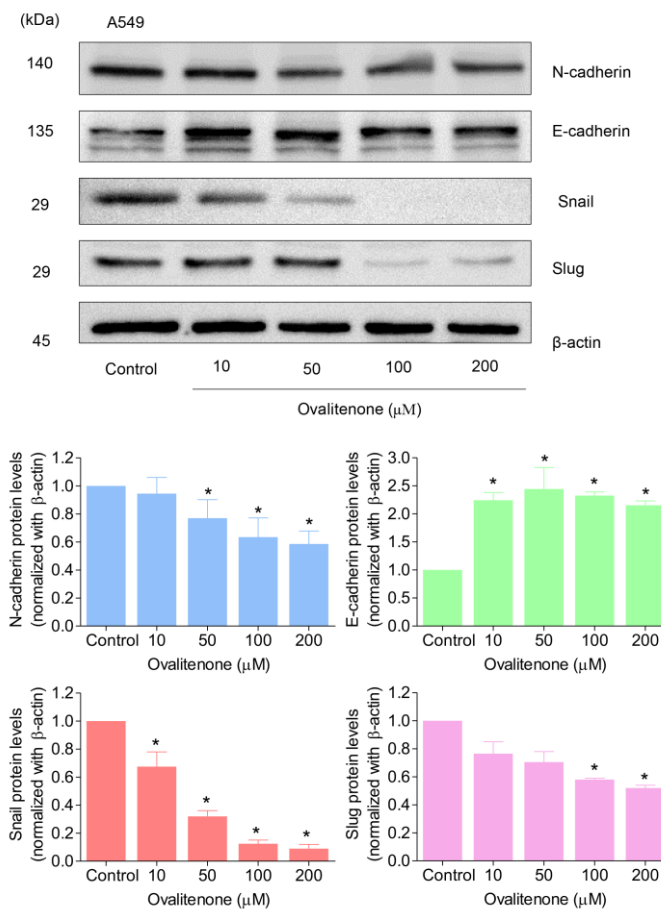


Figure 21 Effect of ovalitenone on epithelial-to-mesenchymal transition (EMT) markers in H460 cells.

After cells treated with non-toxic concentrations of ovalitenone for 24 h, the expression levels of N-cadherin, Snail and Slug were determined by Western blotting. All data are represented by mean  $\pm$  SEM (n = 3). \* $p < 0.05$  compared with untreated cells.

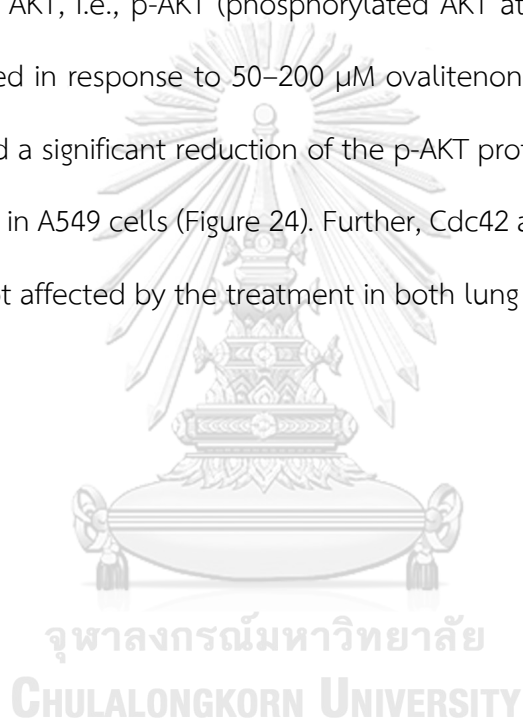




**Figure 22 Effect of ovalitenone on epithelial-to-mesenchymal transition (EMT) markers in A549 cells.**

After cells treated with non-toxic concentrations of ovalitenone for 24 h, the expression levels of N-cadherin, Snail and Slug were determined by Western blotting. All data are represented by mean  $\pm$  SEM (n = 3). \* $p < 0.05$  compared with untreated cells.

Moreover, the upstream regulatory cell signals of EMT and the controllers of cell migration, such as FAK, AKT, mTOR, and Cdc42, were further analyzed. Cdc42 has been implicated as playing an important role in the formation of filopodia, and the level of the protein has also been linked with increased migration <sup>(97)</sup>. The results revealed that ovalitenone was able to decrease the active form of mTOR, i.e., p-mTOR (phosphorylated at Ser2448), in H460 and A549 cells at 50–200  $\mu\text{M}$  ( $p < 0.05$ ). Likewise, the active form of AKT, i.e., p-AKT (phosphorylated AKT at Ser473), was found to be significantly reduced in response to 50–200  $\mu\text{M}$  ovalitenone in H460 cells (Figure 23); however, we found a significant reduction of the p-AKT protein only at concentrations of 100 and 200  $\mu\text{M}$  in A549 cells (Figure 24). Further, Cdc42 and p-FAK (phosphorylated at Tyr397) were not affected by the treatment in both lung cancer cells (Figure 23-24).



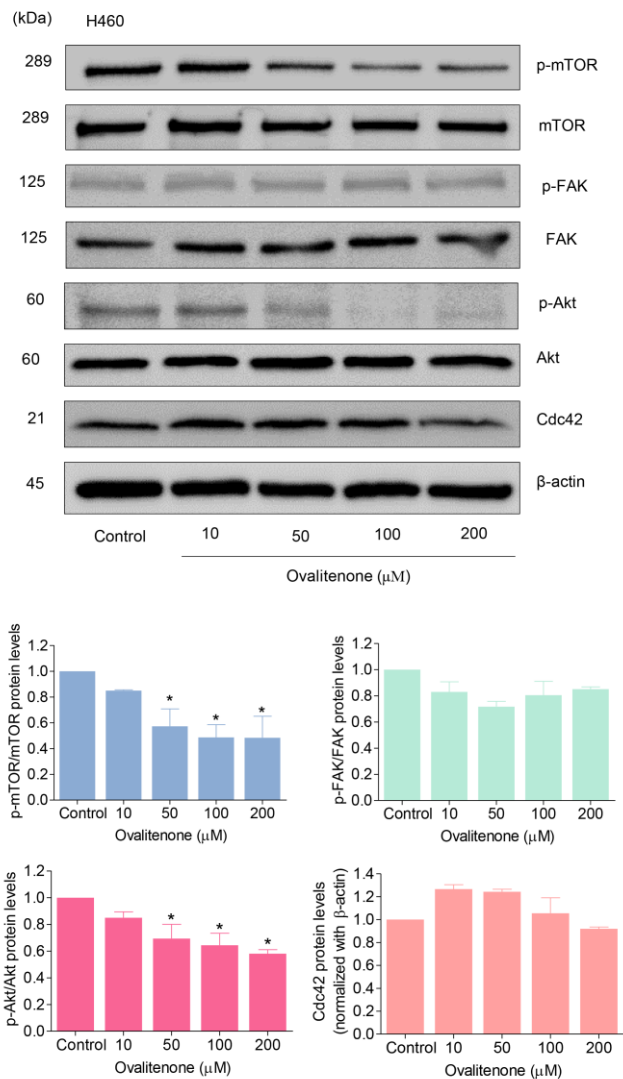


**Figure 23** Ovalitenone suppresses epithelial-to-mesenchymal transition (EMT) through inhibition of the ATP-dependent tyrosine kinase (AKT)/mammalian target of rapamycin (mTOR) signaling pathway in H460 cells.

Levels of phosphorylated mTOR (Ser2448), phosphorylated focal adhesion kinase (FAK) (Tyr397), phosphorylated Akt (Ser473), and Cdc42 were determined by Western blot analysis. All data are represented by mean  $\pm$  SEM (n = 3). \* $p$  < 0.05 compared with untreated cells.

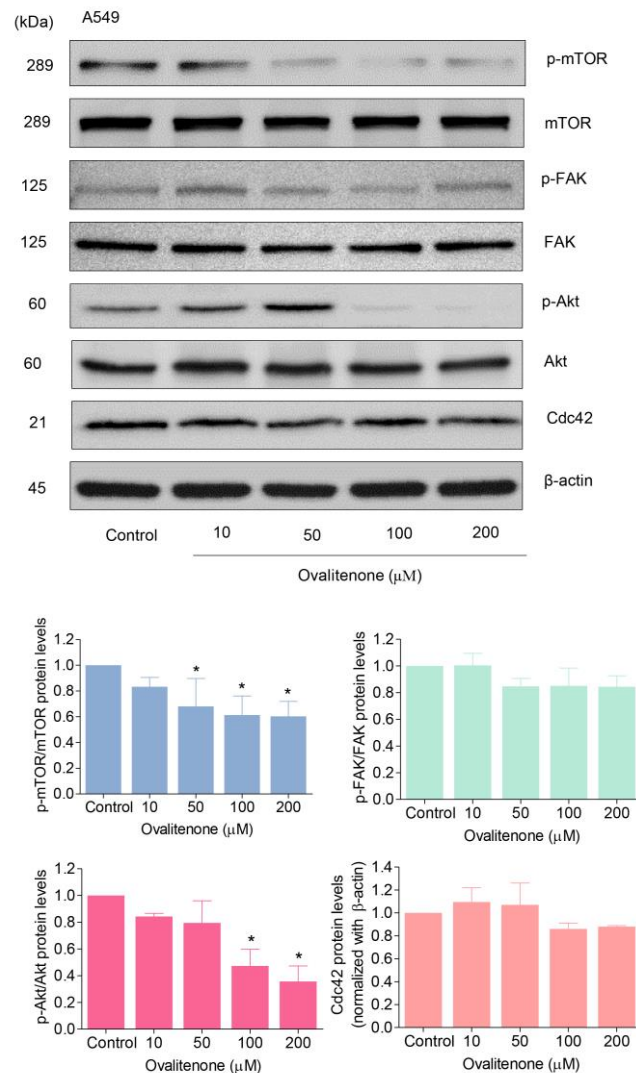


**Figure 24** Ovalitenone suppresses epithelial-to-mesenchymal transition (EMT) through inhibition of the ATP-dependent tyrosine kinase (AKT)/mammalian target of rapamycin (mTOR) signaling pathway in A549 cells.

Levels of phosphorylated mTOR (Ser2448), phosphorylated focal adhesion kinase (FAK) (Tyr397), phosphorylated Akt (Ser473), and Cdc42 were determined by Western blot analysis. All data are represented by mean  $\pm$  SEM ( $n = 3$ ). \* $p < 0.05$  compared with untreated cells.

To confirmed the effect of ovalitenone on E-cadherin, N-cadherin, and snail by immunofluorescence staining. Figure 25-27 shows that ovalitenone significantly decreased the levels of N-cadherin and snail, whereas its dramatically up-regulated E-cadherin in H460 cells. Consistently, similar results from the immunofluorescence analysis in A549 cells were found, as shown in Figure 28-30. These results indicated that ovalitenone suppressed EMT as well as inhibited lung cancer cell motility through inhibition of the AKT/mTOR signaling pathway.

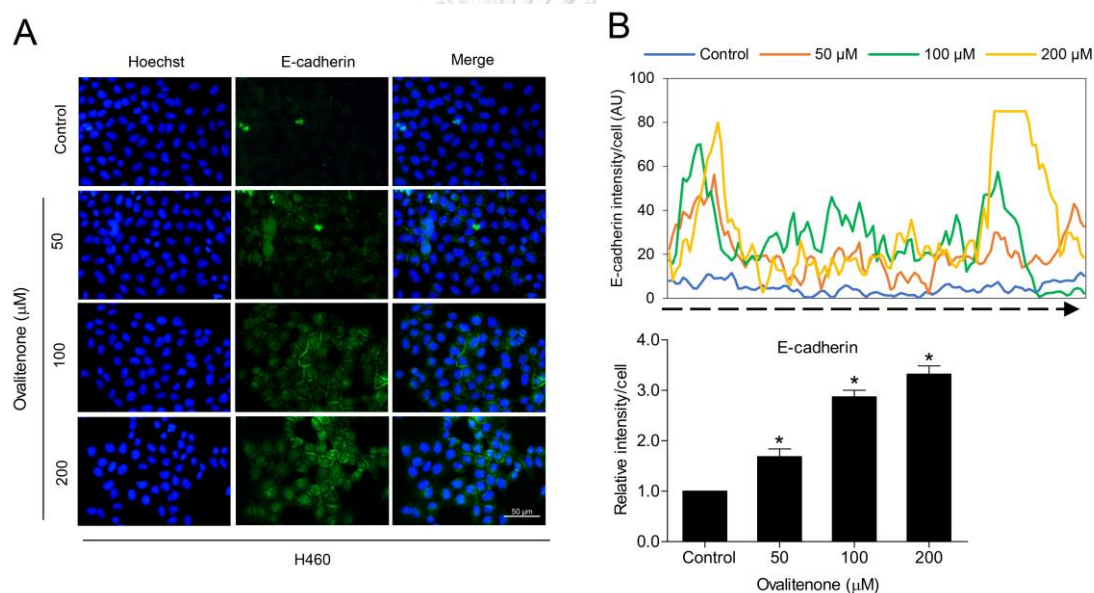


**Figure 25 Ovalitenone increase E-cadherin in H460 cells.**

(A) H460 cells were treated with non-toxic concentrations of ovalitenone for 24 h. The cells were co-stained with anti-E-cadherin antibodies, and Hoechst 33342. The expression of E-cadherin was examined using immunofluorescence. (B) The fluorescence intensity was analyzed by ImageJ software. Values represent the mean  $\pm$  SEM. (n = 3). \* $p < 0.05$  compared with untreated cells.

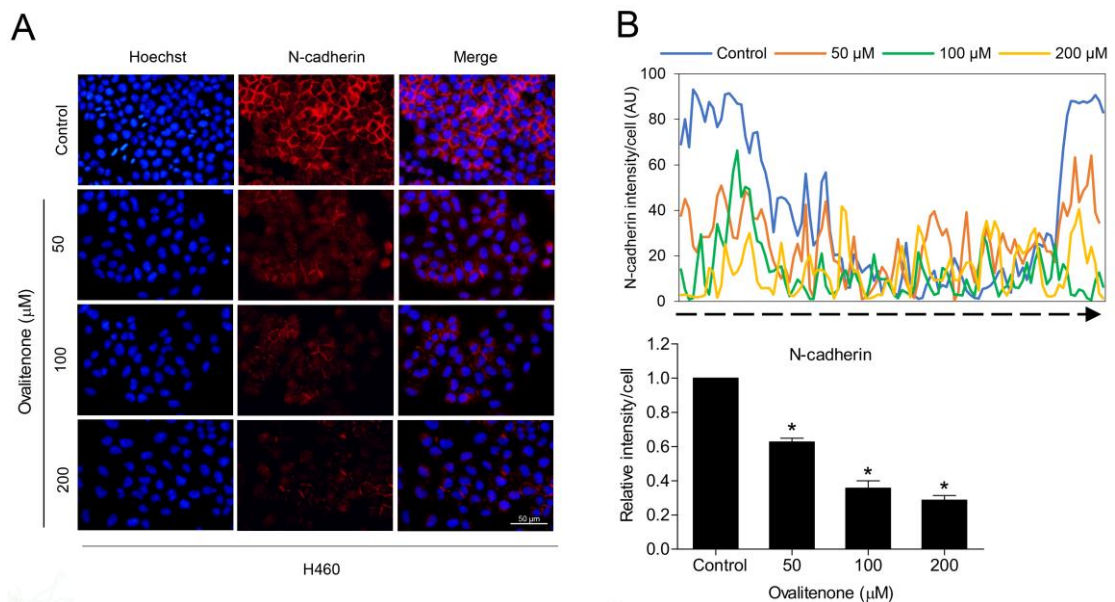


**Figure 26 Ovalitenone suppress N-cadherin in H460 cells.**

(A) H460 cells were treated with non-toxic concentrations of ovalitenone for 24 h. The cells were co-stained with anti-N-cadherin antibodies, and Hoechst 33342. The expression of N-cadherin was examined using immunofluorescence. (B) The fluorescence intensity was analyzed by ImageJ software. Values represent the mean  $\pm$  SEM. (n = 3). \* $p < 0.05$  compared with untreated cells.

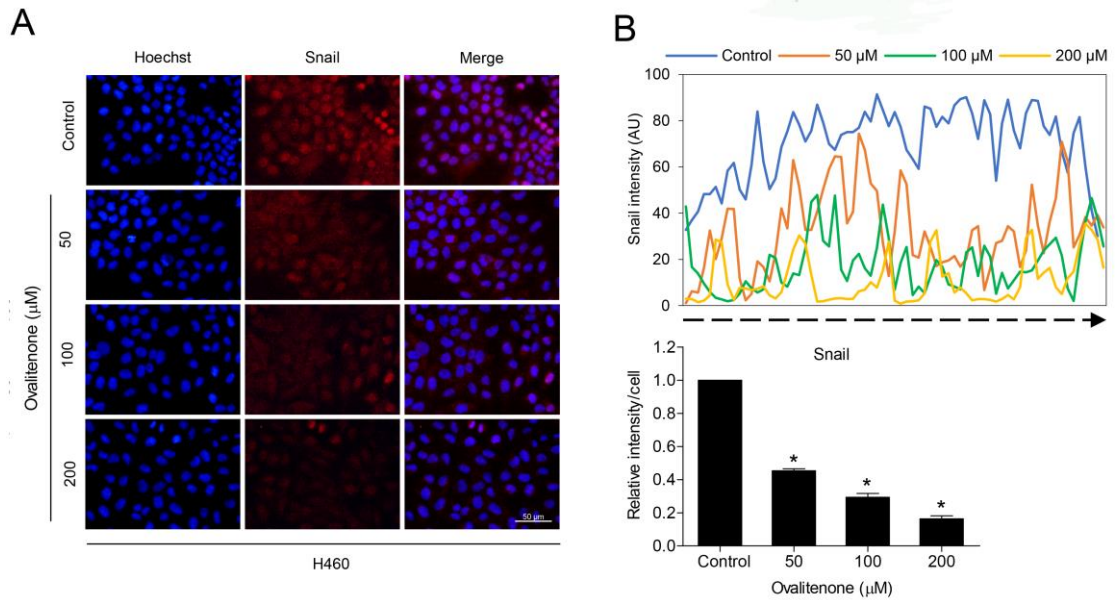


**Figure 27** Ovalitenone suppress Snail in H460 cells.

(A) H460 cells were treated with non-toxic concentrations of ovalitenone for 24 h. The cells were co-stained with anti-Snail antibodies, and Hoechst 33342. The expression of Snail was examined using immunofluorescence. (B) The fluorescence intensity was analyzed by ImageJ software. Values represent the mean  $\pm$  SEM. ( $n = 3$ ).  $*p < 0.05$  compared with untreated cells.

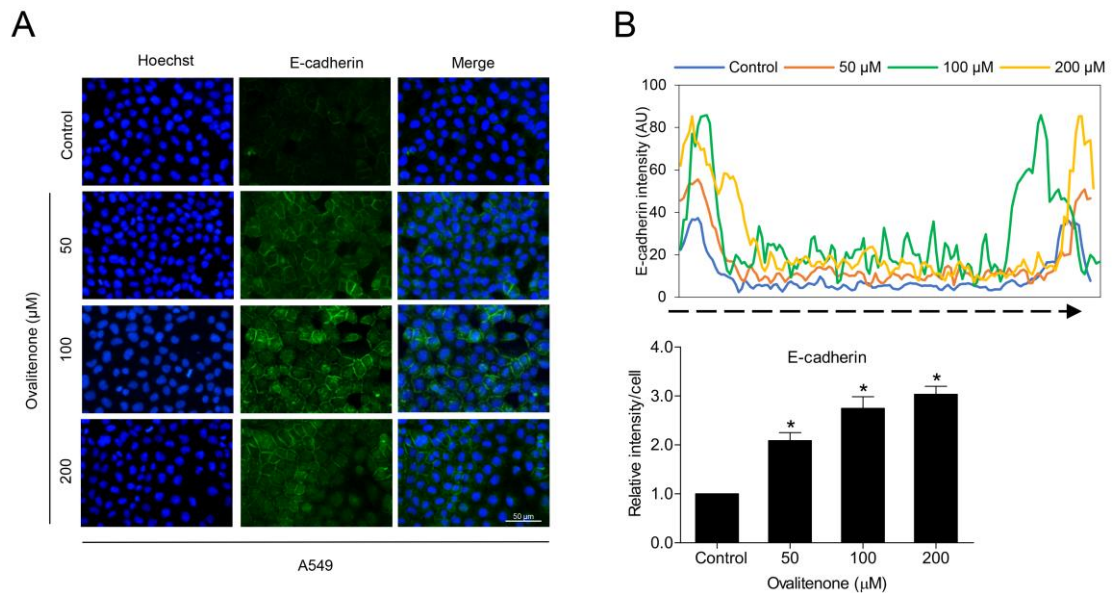


**Figure 28** Ovalitenone increase E-cadherin in A549 cells.

(A) A549 cells were treated with ovalitenone at indicated concentrations for 24 h. The cellular level of E-cadherin was determined by immunofluorescence analysis. (B) The fluorescence intensity was analyzed by ImageJ software. Values represent the mean  $\pm$  SEM. (n = 3). \* $p < 0.05$  compared with untreated cells.



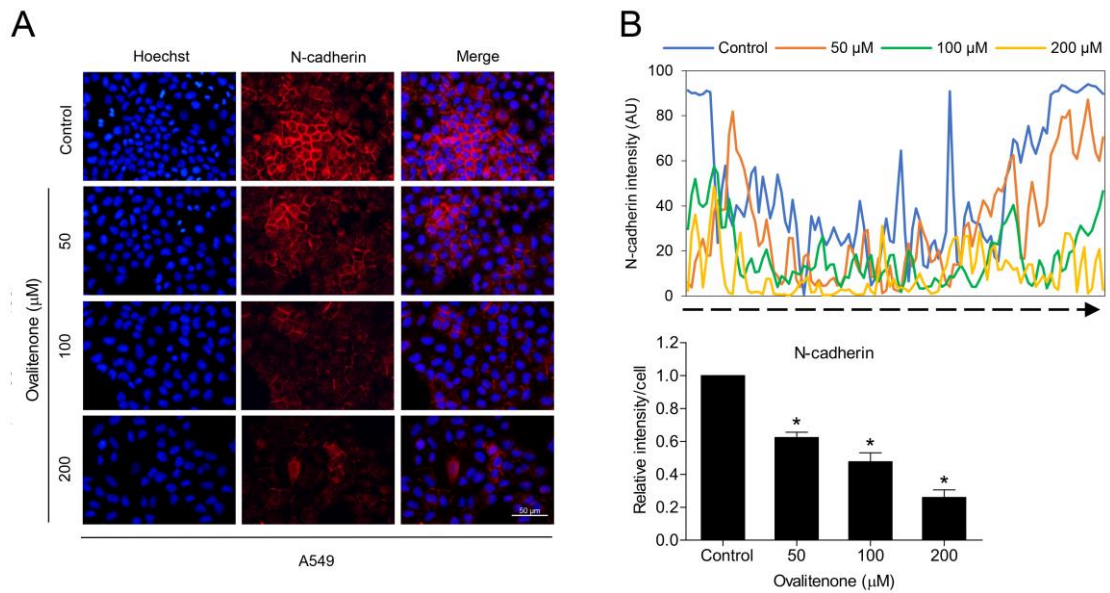


**Figure 29 Ovalitenone suppress N-cadherin in A549 cells.**

(A) A549 cells were treated with ovalitenone at indicated concentrations for 24 h. The cellular level of N-cadherin was determined by immunofluorescence analysis. (B) The fluorescence intensity was analyzed by ImageJ software. Values represent the mean  $\pm$  SEM. (n = 3). \* $p < 0.05$  compared with untreated cells.

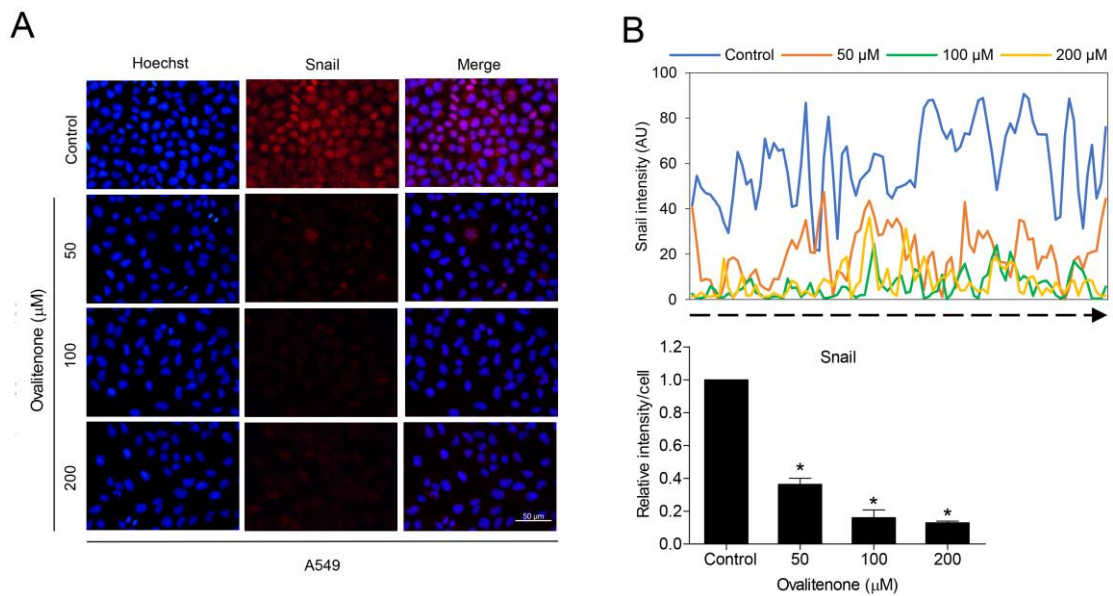


**Figure 30 Ovalitenone suppress Snail in A549 cells.**

(A) A549 cells were treated with ovalitenone at indicated concentrations for 24 h. The cellular level of Snail was determined by immunofluorescence analysis. (B) The fluorescence intensity was analyzed by ImageJ software. Values represent the mean  $\pm$  SEM. (n = 3). \* $p < 0.05$  compared with untreated cells.

## CHAPTER IV

### DISCUSSION AND CONCLUSION

Human lung cancer has been shown to be the leading cause of cancer-related deaths worldwide <sup>(2)</sup>. Cancer cell migration is one of the cancer hallmarks and is critical for the success of metastasis <sup>(82)</sup>. Currently, the 5-year survival of lung cancer with metastasis is considered very low (approximately 18%). However, as most lung cancer patients present with metastatic disease at the first diagnosis <sup>(98)</sup>. As metastasis has been shown to be an important factor of cancer death in lung cancer, approaches that attenuate the metastasis potential are of interest as promising means to improve the clinical outcome. In fact, cancer metastasis is a complex process involving the spread of cancer cells from a primary tumor to different sites of the body through the blood and lymphatic vessels <sup>(4)</sup>. During the process of metastasis, cancer cells must gain the ability to migrate and invade cells, resist detachment-induced apoptosis (anoikis), survive in the circulatory systems, and establish new colonies at metastatic sites <sup>(99)</sup>.

EMT, a switching process from the epithelial phenotype of an adherent cell to a motile mesenchymal phenotype is known to facilitate cancer metastasis in several human cancers <sup>(100)</sup>. Besides, EMT has been highlighted as an important target of anti-cancer drugs as well as a key treatment strategy <sup>(101)</sup>. Numerous studies shown that natural product-derived compounds exhibit potential activities in the inhibition of cancer cell migration and invasion, as well as EMT. For instance, gigantol, a bibenzyl compound extracted from *Dendrobium draconis*, has been shown to suppress EMT in non-small cell lung cancer H460 cells <sup>(102)</sup>. Petpiroon et al. reported that phoyunnanin E inhibits the motility of lung cancer cells via the suppression of EMT and cancer metastasis-related integrins, such as integrin  $\alpha v$  and integrin  $\beta 3$  <sup>(103)</sup>. Furthermore,

ephemeranthol A, a natural compound isolated from *D. infundibulum*, also exhibited inhibitory effects on migration and EMT via inhibition of the FAK-AKT signaling pathway<sup>(104)</sup>. Similarly, batatasin III was reported to have an inhibitory effect on cancer migration and invasion by suppressing EMT<sup>(105)</sup>.

Cell migration through tissues results from a highly integrated multistep process that is regulated by various signaling molecules, such as Rho-GTPases, and focal adhesion kinase (FAK)<sup>(19), (20)</sup>. Focal adhesion kinase (FAK) is an intracellular protein-tyrosine kinase (PTK) involved in the regulation of cell cycle progression, survival, and migration. The ability of cancer cells to migrate has been found to be linked to increased FAK expression, phosphorylation, and catalytic activity<sup>(23)</sup>. The phosphorylation of Y397 of FAK has been reported to play a crucial role in FAK-mediated cell migration<sup>(24)</sup>. Studies have shown the potential anti-migration benefit of FAK/AKT inhibition. Plaibua et al. reported that artonin E inhibits cell migration and invasion via a FAK-AKT-dependent mechanism<sup>(106)</sup>. Cardamonin has also been shown to inhibit cancer metastasis by suppressing the PI3K/AKT/mTOR pathway<sup>(107)</sup>. Focusing on AKT, it was shown that AKT and its related cellular pathways were highly activated in migrating cells<sup>(108)</sup>. In general, AKT is known to be a central signaling pathway for several cell behaviors, such as proliferation, survival, and motility<sup>(70)</sup>. Studies have shown that the activated AKT plays an important role in cancer cell metastasis and the EMT process<sup>(109)</sup>.

AKT can activate mTOR through the direct phosphorylation of tuberous sclerosis complex 2 (TSC2)<sup>(110)</sup>. mTOR is a molecule downstream of the AKT pathway that has been shown to regulate a series of critical cellular metabolism, migration, invasion, and angiogenesis<sup>(111)</sup>. In the present study, we assessed the expression of

proteins and found that ovalitenone could inhibit the active AKT and mTOR, which could at least in part be responsible for the anti-migration activity of the compound. The regulatory link between AKT/mTOR and EMT has been revealed in several studies. One study shown that transforming growth factor beta (TGF- $\beta$ ) induced EMT and cell invasion via the activation of mTORC2 kinase activity <sup>(112)</sup>. Moreover, mTORC1 and mTORC2 were shown to be modulators of EMT in cancer, while the silencing mTORC1 and mTORC2 resulted in an increase in E-cadherin and decrease in N-cadherin, Vimentin, and Snail, and other characteristics of mesenchymal to epithelial transition (MET) <sup>(113)</sup>.

Recently, CSCs, a small groups of cancer cells within tumors having stem cell properties, were shown to be implicated in the initiation, progression, metastasis, and recurrence of lung cancer <sup>(114)</sup>. The characteristics of CSCs include a renewal ability, differentiation, high invasiveness, and resistance to chemotherapy. CSCs are the main factor contributing to the current low rate of therapeutic success <sup>(115)</sup>. According to the data, CSCs are considered to be the critical driver of cancer aggressiveness, including high tumor maintenance, the probability of metastasis, avoidance of the immune system, resistance to chemotherapy, and cancer relapse <sup>(116)</sup>. Interestingly, our results suggest a potential role of ovalitenone in the inhibition of CSCs, as the treatment of lung cancer cells at non-toxic concentrations could significantly decrease the ability to form tumor spheroids (Figure 19-20). The ability of a single cancer cell to generate a growing tumor spheroid has been used for CSC assessment in many research studies <sup>(117), (118)</sup>. Besides, the regulatory pathways that are widely accepted to regulate and maintain CSCs in cancers, including the AKT and mTOR signals, were suppressed by the treatment of ovalitenone (Figure 23-24). AKT and mTOR were demonstrated to be

critical cell signaling pathways for CSC maintenance in many cancers, including lung cancer <sup>(119)</sup>. Moreover, strategies that target these pathways have been shown to be promising approaches for lung cancer treatment <sup>(120)</sup>. EMT and CSCs were shown to be involved in a close crosstalk network. In some studies, EMT was shown to increase CSC phenotypes in cancers <sup>(121)</sup>. The association between EMT and CSC formation is an important process that drives cancer progression, drug resistance, and cancer metastasis <sup>(122)</sup>. Interestingly, EMT transcription factors, including snail, twist, and ZEB families, are also known to confer multiple CSC properties <sup>(123)</sup>.

The lung cancer cells H460 and A549 cells were used as cell models in the present study. The H460 and A549 cells have Kras mutations, which was shown to associate with metastatic potentials <sup>(124), (125)</sup>. In lung cancer, Ras mutations are found in around 32%, Kras being the most common member of the mutated family <sup>(126)</sup>. Kras protein, a small guanine triphosphatase (GTPase), functions in the transducing signal of receptor epidermal growth factor receptor (EGFR) and tyrosine kinases. Moreover, Ras proteins recruit and activate downstream effectors, such as AKT and ERK pathways that in turn affect cell growth, differentiation and survival <sup>(127)</sup>. As we focus on the EMT process, Kras is known to activate EMT, resulting in tumor progression and metastasis. Kras mutations were shown to induce EMT through several mechanisms including the upregulation of the EMT transcription factors, Snail and Slug <sup>(128)</sup>. In terms of cell migration, several studies have utilized both H460 and A549 cell lines for investigating migratory activity and anti-migratory investigation of lung cancer cells. For instance, Xia Rongmu et al. demonstrated the anti-migration and anti-invasion of hesperidin in A549 cells <sup>(129)</sup>. Lv Xiao-qin et al. used H460 and A549 cells as models for studying the inhibitory effects of Honokiol on EMT-mediated motility and migration <sup>(130)</sup>.

Furthermore, Ophiopogonin B was shown to suppresses metastasis-related activities of A549 cells <sup>(131)</sup>.

Recently, natural compounds from plants have been receiving increasing attention either as the potential drugs or lead compounds in drug discovery <sup>(132)</sup>. *Millettia erythrocalyx*, which is widely distributed in the tropical and subtropical regions of the world, such as China and Thailand <sup>(33)</sup>, is one natural species that has attracted interest and is a source of ovalitenone. Ovalitenone was isolated from *M. erythrocalyx* has been used in various traditional medicines, such as for treating bleeding piles, fistulous sores, bronchitis, and coughs <sup>(36)</sup>. Here, we found that ovalitenone inhibited cell migration and invasion, as well as EMT in human lung cancer H460 and A549 cells. Ovalitenone suppressed the formation of cancer cell colonies and cancer cell spheroids in terms of the number and size of the colonies and spheroids (Figure 18-20). Moreover, the treatment of human lung cancer cells with ovalitenone at non-toxic concentrations significantly decreased the levels of N-cadherin, snail, and slug, while it increased E-cadherin (Figure 21-22), indicating the effect of this compound in terms of its inhibition of EMT; thereby, resulting in the inhibition of cell movement from the suppression of the AKT/mTOR pathways (Figure 23-24).

In conclusion, showing that ovalitenone compound was able to inhibits cancer migration and invasion, and anchorage-independent growths. The results demonstrated that ovalitenone suppressed EMT and AKT/mTOR signals pathway, which are important controllers of cancer cell migration, invasion, and metastasis (Figure 31). In addition to ovalitenone could reduce CSC-like phenotypes formation in lung cancer cells. These data could support the development of ovalitenone treatment for anti-metastatic therapy.

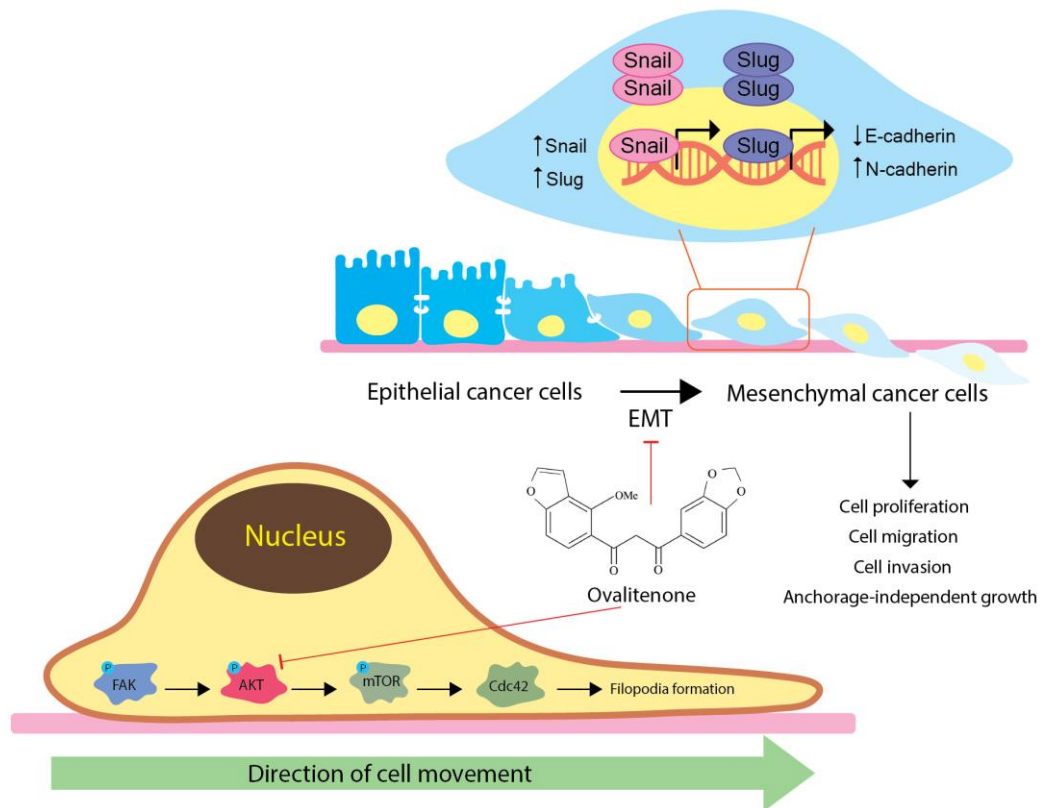


Figure 31 The schematic diagram summarizes the underlying mechanism of ovalitenone-attenuating EMT in lung cancer.



**APPENDIX**  
**PREPARATION OF REAGENTS**

1. DMEM stock solution (1 L)

DMEM powder	10.4 g
NaHCO <sub>3</sub>	3.7 g
ddH <sub>2</sub> O	950 mL

Adjust pH to 7.2 with 1 N HCl or 1 N NaOH

Add ddH<sub>2</sub>O to 1 L and sterilized by filtering through a 0.2 sterile membrane filter

Store at 4 °C

2. RPMI 1640 stock solution (1 L)

RPMI powder	10.4 g
NaHCO <sub>3</sub>	2.0 g
Glucose	4.5 g
Sodium pyruvate	0.11 g
HEPES (1M)	10 mL
ddH <sub>2</sub> O	950 mL

Adjust pH to 7.2 with 1 N HCl and 1 N NaOH

Add ddH<sub>2</sub>O to 1 L and sterilized by filtering through a 0.2 sterile membrane filter

3. Separating buffer (500 mL)

Tris base	45.43 g
ddH <sub>2</sub> O	450 mL

Adjust pH to 8.8 with 1 N HCl or 1 N NaOH

Add ddH<sub>2</sub>O to 500 mL

4. Stacking buffer (500 mL)

Tris base 15.14 g

ddH<sub>2</sub>O 450 mL

5. TBS (1000 mL)

1 M Tris-HCl (pH 7.5) 20 mL

5 M NaCl 27.5 mL

Add ddH<sub>2</sub>O to 1000 mL

6. TBS-T (1000 mL)

1 M Tris-HCl (pH 7.5) 20 mL

5 M NaCl 27.5 mL

Tween-20 1 mL

Add ddH<sub>2</sub>O to 1000 mL

7. 5 M NaCl (100 mL)

NaCl 29.22 g

ddH<sub>2</sub>O 100 mL

8. 10% SDS (10 mL)

SDS 1 g

ddH<sub>2</sub>O 10 mL

9. 6× Loading Buffer (10 mL)

4× Tris-HCl SDS pH 6.8 7 mL

Glycerol 3 mL

SDS 1 g



Bromophenol blue 1.2 mg

2-mercaptol ethanol 0.42 mL

Make small aliquot store at  $-20^{\circ}\text{C}$



## REFERENCES

1. Jemal A, Bray F, Center MM, Ferlay J, Ward E, Forman DJ. Global cancer statistics. 2011;61(2):69-90.
2. Bray F, Ferlay J, Soerjomataram I, Siegel RL, Torre LA, Jemal A. Global cancer statistics 2018: GLOBOCAN estimates of incidence and mortality worldwide for 36 cancers in 185 countries. 2018;68(6):394-424.
3. Guan X. Cancer metastases: challenges and opportunities. *Acta pharmaceutica sinica B*. 2015;5(5):402-18.
4. Karlsson MC, Gonzalez SF, Welin J, Fuxe J. Epithelial-mesenchymal transition in cancer metastasis through the lymphatic system. *Molecular oncology*. 2017;11(7):781-91.
5. Sun M, Liu X-H, Wang K-M, Nie F-q, Kong R, Yang J-s, et al. Downregulation of BRAF activated non-coding RNA is associated with poor prognosis for non-small cell lung cancer and promotes metastasis by affecting epithelial-mesenchymal transition. *Molecular cancer*. 2014;13(1):1-12.
6. Tiwari N, Gheldof A, Tataru M, Christofori G, editors. EMT as the ultimate survival mechanism of cancer cells. *Seminars in cancer biology*; 2012: Elsevier.
7. Weber GF. Why does cancer therapy lack effective anti-metastasis drugs? *Cancer letters*. 2013;328(2):207-11.
8. Anderson RL, Balasas T, Callaghan J, Coombes RC, Evans J, Hall JA, et al. A framework for the development of effective anti-metastatic agents. *Nature Reviews Clinical Oncology*. 2019;16(3):185-204.
9. Sosa Iglesias V, Giuranno L, Dubois LJ, Theys J, Vooijs M. Drug resistance in non-small cell lung cancer: a potential for NOTCH targeting? *Frontiers in oncology*. 2018;8:267.
10. Fidler I. Cancer metastasis. *British medical bulletin*. 1991;47(1):157-77.
11. HARLOZINSKA A. Progress in molecular mechanisms of tumor metastasis and angiogenesis. *Anticancer research*. 2005;25(5):3327-33.
12. Voulgari A, Pintzas A. Epithelial-mesenchymal transition in cancer metastasis: mechanisms, markers and strategies to overcome drug resistance in the clinic. *Biochimica et Biophysica Acta (BBA)-Reviews on Cancer*. 2009;1796(2):75-90.
13. Kim Y-N, Koo KH, Sung JY, Yun U-J, Kim H. Anoikis resistance: an essential prerequisite for tumor metastasis. *International journal of cell biology*. 2012;2012.

14. Scanlon C, Van Tubergen E, Inglehart R, D'silva N. Biomarkers of epithelial-mesenchymal transition in squamous cell carcinoma. *Journal of dental research*. 2013;92(2):114-21.
15. Hazan RB, Qiao R, Keren R, Badano I, Suyama K. Cadherin switch in tumor progression. *Annals of the New York Academy of Sciences*. 2004;1014(1):155-63.
16. Peinado H, Portillo F, Cano A. Transcriptional regulation of cadherins during development and carcinogenesis. *International Journal of Developmental Biology*. 2004;48(5-6):365-75.
17. Shah PP, Kakar SS. Pituitary tumor transforming gene induces epithelial to mesenchymal transition by regulation of Twist, Snail, Slug, and E-cadherin. *Cancer letters*. 2011;311(1):66-76.
18. Lamouille S, Xu J, Derynck R. Molecular mechanisms of epithelial-mesenchymal transition. *Nature reviews Molecular cell biology*. 2014;15(3):178-96.
19. Ridley AJ. Rho GTPases and cell migration. *Journal of cell science*. 2001;114(15):2713-22.
20. Meng X, Jin Y, Yu Y, Bai J, Liu G, Zhu J, et al. Characterisation of fibronectin-mediated FAK signalling pathways in lung cancer cell migration and invasion. *British journal of cancer*. 2009;101(2):327-34.
21. Ridley AJ, Schwartz MA, Burridge K, Firtel RA, Ginsberg MH, Borisy G, et al. Cell migration: integrating signals from front to back. *Science*. 2003;302(5651):1704-9.
22. Lechertier T, Hoidalva-Dilke K. Focal adhesion kinase and tumour angiogenesis. *The Journal of pathology*. 2012;226(2):404-12.
23. Schaller MD. Cellular functions of FAK kinases: insight into molecular mechanisms and novel functions. *Journal of cell science*. 2010;123(7):1007-13.
24. Schlaepfer DD, Mitra SK, Ilic D. Control of motile and invasive cell phenotypes by focal adhesion kinase. *Biochimica et Biophysica Acta (BBA)-Molecular Cell Research*. 2004;1692(2-3):77-102.
25. LoPiccolo J, Granville CA, Gills JJ, Dennis PA. Targeting Akt in cancer therapy. *Anti-cancer drugs*. 2007;18(8):861-74.
26. Kennedy SG, Kandel ES, Cross TK, Hay N. Akt/Protein kinase B inhibits cell death by preventing the release of cytochrome c from mitochondria. *Molecular and cellular biology*. 1999;19(8):5800-10.
27. Zhou H, Huang S. Role of mTOR signaling in tumor cell motility, invasion and metastasis. *Current Protein and Peptide Science*. 2011;12(1):30-42.

28. Baek SH, Ko JH, Lee JH, Kim C, Lee H, Nam D, et al. Ginkgolic acid inhibits invasion and migration and tgf- $\beta$ -induced emt of lung cancer cells through pi3k/akt/mtor inactivation. *Journal of cellular physiology*. 2017;232(2):346-54.
29. Sinha S, Yang W. Cellular signaling for activation of Rho GTPase Cdc42. *Cellular signalling*. 2008;20(11):1927-34.
30. Tian Y, Li M, Song W, Jiang R, Li YQ. Effects of probiotics on chemotherapy in patients with lung cancer. *Oncology letters*. 2019;17(3):2836-48.
31. Housman G, Byler S, Heerboth S, Lapinska K, Longacre M, Snyder N, et al. Drug resistance in cancer: an overview. *Cancers*. 2014;6(3):1769-92.
32. Seca AM, Pinto DC. Plant secondary metabolites as anticancer agents: successes in clinical trials and therapeutic application. *International journal of molecular sciences*. 2018;19(1):263.
33. Jin S, Oh YN, Son YR, Choi SM, Kwon HJ, Kim BW. Antioxidative and Anticancer Activities of Ethanol Extract of *Millettia erythrocalyx*. *Journal of Life Science*. 2018;28(1):50-7.
34. Sritularak B, Likhitwitayawuid K, Conrad J, Kraus W. Flavonoids from the roots of *Millettia erythrocalyx*. *Phytochemistry*. 2002;61(8):943-7.
35. Pooja A, Arun N, Maninder K. Screening of plant essential oils for antifungal activity against *Malassezia furfur*. *International Journal of Pharmacy and Pharmaceutical Sciences*. 2013;5(2):37-9.
36. Rahman MS, Begum B, Chowdhury R, Rahman KM, Rashid MA. Preliminary cytotoxicity screening of some medicinal plants of Bangladesh. *Dhaka University Journal of Pharmaceutical Sciences*. 2008;7(1):47-52.
37. Sharma R, Vishwakarma RA, Bharate SB. An efficient transformation of furano-hydroxychalcones to furanoflavones via base mediated intramolecular tandem O-arylation and C–O bond cleavage: a new approach for the synthesis of furanoflavones. *Organic & Biomolecular Chemistry*. 2015;13(42):10461-5.
38. Likhitwitayawuid K, Sritularak B, Benchanak K, Lipipun V, Mathew J, Schinazi RF. Phenolics with antiviral activity from *Millettia erythrocalyx* and *Artocarpus lakoocha*. *Natural Product Research*. 2005;19(2):177-82.
39. Travis WD, Brambilla E, Nicholson AG, Yatabe Y, Austin JH, Beasley MB, et al. The 2015 World Health Organization classification of lung tumors: impact of genetic, clinical and radiologic advances since the 2004 classification. *Journal of thoracic oncology*. 2015;10(9):1243-60.
40. Zappa C, Mousa SA. Non-small cell lung cancer: current treatment and future advances. *Translational lung cancer research*. 2016;5(3):288.

41. Rossi G, Pelosi G, Barbareschi M, Graziano P, Cavazza A, Papotti M. Subtyping Non–Small Cell Lung Cancer: Relevant Issues and Operative Recommendations for the Best Pathology Practice. *International journal of surgical pathology*. 2013;21(4):326-36.
42. O’Keeffe LM, Taylor G, Huxley RR, Mitchell P, Woodward M, Peters SA. Smoking as a risk factor for lung cancer in women and men: a systematic review and meta-analysis. *BMJ open*. 2018;8(10):e021611.
43. Ridge CA, McErlean AM, Ginsberg MS, editors. *Epidemiology of lung cancer. Seminars in interventional radiology*; 2013: Thieme Medical Publishers.
44. Malhotra J, Malvezzi M, Negri E, La Vecchia C, Boffetta P. Risk factors for lung cancer worldwide. *European Respiratory Journal*. 2016;48(3):889-902.
45. Minna JD, Roth JA, Gazdar AF. Focus on lung cancer. *Cancer cell*. 2002;1(1):49-52.
46. Collins LG, Haines C, Perkel R, Enck RE. Lung cancer: diagnosis and management. *American family physician*. 2007;75(1):56-63.
47. Mirsadraee S, Oswal D, Alizadeh Y, Caulo A, van Beek EJ. The 7th lung cancer TNM classification and staging system: Review of the changes and implications. *World journal of radiology*. 2012;4(4):128.
48. Latimer K, Mott T. Lung cancer: diagnosis, treatment principles, and screening. *American family physician*. 2015;91(4):250-6.
49. Lo C, Zimmermann C, Rydall A, Walsh A, Jones JM, Moore MJ, et al. Longitudinal study of depressive symptoms in patients with metastatic gastrointestinal and lung cancer. *J Clin Oncol*. 2010;28(18):3084-9.
50. Hopwood P, Stephens R. Symptoms at presentation for treatment in patients with lung cancer: implications for the evaluation of palliative treatment. *British journal of cancer*. 1995;71(3):633-6.
51. Khalid U, Spiro A, Baldwin C, Sharma B, McGough C, Norman A, et al. Symptoms and weight loss in patients with gastrointestinal and lung cancer at presentation. *Supportive care in cancer*. 2007;15(1):39.
52. Huang C-Y, Ju D-T, Chang C-F, Reddy PM, Velmurugan BK. A review on the effects of current chemotherapy drugs and natural agents in treating non–small cell lung cancer. *Biomedicine*. 2017;7(4).
53. Hirsch FR, Scagliotti GV, Mulshine JL, Kwon R, Curran Jr WJ, Wu Y-L, et al. Lung cancer: current therapies and new targeted treatments. *The Lancet*. 2017;389(10066):299-311.

54. Lemjabbar-Alaoui H, Hassan OU, Yang Y-W, Buchanan P. Lung cancer: Biology and treatment options. *Biochimica et Biophysica Acta (BBA)-Reviews on Cancer*. 2015;1856(2):189-210.
55. Arany I, Safirstein RL, editors. *Cisplatin nephrotoxicity. Seminars in nephrology*; 2003: Elsevier.
56. Miller RP, Tadagavadi RK, Ramesh G, Reeves WB. Mechanisms of cisplatin nephrotoxicity. *Toxins*. 2010;2(11):2490-518.
57. Mittal V. Epithelial mesenchymal transition in tumor metastasis. *Annual Review of Pathology: Mechanisms of Disease*. 2018;13:395-412.
58. Yang J, Antin P, Berx G, Blanpain C, Brabletz T, Bronner M, et al. Guidelines and definitions for research on epithelial–mesenchymal transition. *Nature Reviews Molecular Cell Biology*. 2020:1-12.
59. von der Mark K, Schöber S, Goodman SL. Integrins in cell migration. *Integrin Protocols: Springer*; 1999. p. 219-30.
60. Staff A. An introduction to cell migration and invasion. *Scandinavian Journal of Clinical and Laboratory Investigation*. 2001;61(4):257-68.
61. Yamaguchi H, Wyckoff J, Condeelis J. Cell migration in tumors. *Current opinion in cell biology*. 2005;17(5):559-64.
62. Stylli SS, Kaye AH, Lock P. Invadopodia: at the cutting edge of tumour invasion. *Journal of clinical neuroscience*. 2008;15(7):725-37.
63. Zhao X, Guan J-L. Focal adhesion kinase and its signaling pathways in cell migration and angiogenesis. *Advanced drug delivery reviews*. 2011;63(8):610-5.
64. Parsons JT. Focal adhesion kinase: the first ten years. *Journal of cell science*. 2003;116(8):1409-16.
65. Wang B, Qi X, Li D, Feng M, Meng X, Fu S. Expression of pY397 FAK promotes the development of non-small cell lung cancer. *Oncology Letters*. 2016;11(2):979-83.
66. Grisar-Granovsky S, Salah Z, Maoz M, Pruss D, Beller U, Bar-Shavit R. Differential expression of protease activated receptor 1 (Par1) and pY397FAK in benign and malignant human ovarian tissue samples. *International journal of cancer*. 2005;113(3):372-8.
67. Sieg DJ, Hauck CR, Schlaepfer DD. Required role of focal adhesion kinase (FAK) for integrin-stimulated cell migration. *Journal of cell science*. 1999;112(16):2677-91.
68. Sieg DJ, Hauck CR, Ilic D, Klingbeil CK, Schaefer E, Damsky CH, et al. FAK integrates growth-factor and integrin signals to promote cell migration. *Nature cell biology*. 2000;2(5):249-56.



69. Frame MC. Src in cancer: deregulation and consequences for cell behaviour. *Biochimica et Biophysica Acta (BBA)-Reviews on Cancer*. 2002;1602(2):114-30.
70. Stambolic V, Woodgett JR. Functional distinctions of protein kinase B/Akt isoforms defined by their influence on cell migration. *Trends in cell biology*. 2006;16(9):461-6.
71. Grille SJ, Bellacosa A, Upson J, Klein-Szanto AJ, Van Roy F, Lee-Kwon W, et al. The protein kinase Akt induces epithelial mesenchymal transition and promotes enhanced motility and invasiveness of squamous cell carcinoma lines. *Cancer research*. 2003;63(9):2172-8.
72. Onishi K, Higuchi M, Asakura T, Masuyama N, Gotoh Y. The PI3K-Akt pathway promotes microtubule stabilization in migrating fibroblasts. *Genes to Cells*. 2007;12(4):535-46.
73. Puchsaka P, Chaotham C, Chanvorachote P.  $\alpha$ -Lipoic acid sensitizes lung cancer cells to chemotherapeutic agents and anoikis via integrin  $\beta 1/\beta 3$  downregulation. *International Journal of Oncology*. 2016;49(4):1445-56.
74. Tan AC. Targeting the PI3K/Akt/mTOR pathway in non-small cell lung cancer (NSCLC). *Thoracic Cancer*. 2020;11(3):511-8.
75. Qiao M, Sheng S, Pardee AB. Metastasis and AKT activation. *Cell cycle*. 2008;7(19):2991-6.
76. Houssaini A, Breau M, Kanny Kebe SA, Marcos E, Lipskaia L, Rideau D, et al. mTOR pathway activation drives lung cell senescence and emphysema. *JCI insight*. 2018;3(3).
77. Tian T, Li X, Zhang J. mTOR signaling in cancer and mTOR inhibitors in solid tumor targeting therapy. *International journal of molecular sciences*. 2019;20(3):755.
78. Fumarola C, Bonelli MA, Petronini PG, Alfieri RR. Targeting PI3K/AKT/mTOR pathway in non small cell lung cancer. *Biochemical pharmacology*. 2014;90(3):197-207.
79. Schmidt A, Hall A. Guanine nucleotide exchange factors for Rho GTPases: turning on the switch. *Genes & development*. 2002;16(13):1587-609.
80. Chen Q-Y, Jiao D-M, Yao Q-H, Yan J, Song J, Chen F-Y, et al. Expression analysis of Cdc42 in lung cancer and modulation of its expression by curcumin in lung cancer cell lines. *International journal of oncology*. 2012;40(5):1561-8.
81. Jiang L, Zhang Y, Qu X. Effects of Cdc42 overexpression on the estrogen-enhanced multidrug resistance in breast cancer cells. *Zhonghua zhong liu za zhi [Chinese journal of oncology]*. 2011;33(7):489-93.

82. Hanahan D, Weinberg RA. Hallmarks of cancer: the next generation. *cell*. 2011;144(5):646-74.
83. Denlinger CE, Ikonomidis JS, Reed CE, Spinale FG. Epithelial to mesenchymal transition: the doorway to metastasis in human lung cancers. Mosby; 2010.
84. Jing Y, Han Z, Zhang S, Liu Y, Wei L. Epithelial-Mesenchymal Transition in tumor microenvironment. *Cell & bioscience*. 2011;1(1):29.
85. Zeisberg M, Kalluri R. The role of epithelial-to-mesenchymal transition in renal fibrosis. *Journal of Molecular Medicine*. 2004;82(3):175-81.
86. Xiao D, He J. Epithelial mesenchymal transition and lung cancer. *Journal of thoracic disease*. 2010;2(3):154.
87. Vergara D, Merlot B, Lucot J-P, Collinet P, Vinatier D, Fournier I, et al. Epithelial-mesenchymal transition in ovarian cancer. *Cancer letters*. 2010;291(1):59-66.
88. Gavert N, Ben-Ze'ev A. Epithelial-mesenchymal transition and the invasive potential of tumors. *Trends in molecular medicine*. 2008;14(5):199-209.
89. Wang Y, Shi J, Chai K, Ying X, P Zhou B. The role of snail in EMT and tumorigenesis. *Current cancer drug targets*. 2013;13(9):963-72.
90. Wu Y, Evers BM, Zhou BP. Small C-terminal domain phosphatase enhances snail activity through dephosphorylation. *Journal of Biological Chemistry*. 2009;284(1):640-8.
91. Legras A, Pécuchet N, Imbeaud S, Pallier K, Didelot A, Roussel H, et al. Epithelial-to-mesenchymal transition and MicroRNAs in lung cancer. *Cancers*. 2017;9(8):101.
92. Sritularak B. Bioactive phenolics from *Artocarpus gomezianus* and *Millettia erythrocalyx*: Chulalongkorn University; 2002.
93. Ganapaty S, Pushpalatha V, Babu GJ, Naidu KC, Waterman PG. Flavonoids from *Millettia peguensis* Ali (Fabaceae). *Biochemical systematics and ecology*. 1998;1(26):125-6.
94. Gupta RK, Krishnamurti M. New dibenzoylmethane and chalcone derivatives from *Millettia ovalifolia* seeds. *Phytochemistry*. 1977.
95. Asomaning WA, Otoo E, Akoto O, Oppong IV, Addae-Mensah I, Waibel R, et al. Isoflavones and coumarins from *Millettia thonningii*. *Phytochemistry*. 1999;51(7):937-41.
96. Mori S, Chang JT, Andrechek ER, Matsumura N, Baba T, Yao G, et al. Anchorage-independent cell growth signature identifies tumors with metastatic potential. *Oncogene*. 2009;28(31):2796-805.
97. Mattila PK, Lappalainen P. Filopodia: molecular architecture and cellular functions. *Nature reviews Molecular cell biology*. 2008;9(6):446-54.

98. David EA, Clark JM, Cooke DT, Melnikow J, Kelly K, Canter RJ. The role of thoracic surgery in the therapeutic management of metastatic non-small cell lung cancer. *Journal of thoracic oncology*. 2017;12(11):1636-45.
99. Liu H, Zhang X, Li J, Sun B, Qian H, Yin Z. The biological and clinical importance of epithelial-mesenchymal transition in circulating tumor cells. *Journal of cancer research and clinical oncology*. 2015;141(2):189-201.
100. Foroni C, Brogini M, Generali D, Damia G. Epithelial-mesenchymal transition and breast cancer: Role, molecular mechanisms and clinical impact. *Cancer treatment reviews*. 2012;38(6):689-97.
101. Ramesh V, Brabletz T, Ceppi P. Targeting EMT in cancer with repurposed metabolic inhibitors. *Trends in Cancer*. 2020.
102. Unahabhokha T, Chanvorachote P, Sritularak B, Kitsongsermthon J, Pongrakhananon V. Gigantol inhibits epithelial to mesenchymal process in human lung cancer cells. *Evidence-Based Complementary and Alternative Medicine*. 2016;2016.
103. Petpiroon N, Sritularak B, Chanvorachote P. Phoyunnanin E inhibits migration of non-small cell lung cancer cells via suppression of epithelial-to-mesenchymal transition and integrin  $\alpha_v$  and integrin  $\beta_3$ . *BMC complementary and alternative medicine*. 2017;17(1):1-16.
104. Nonpanya N, Prakhongcheep O, Petsri K, Jitjaicham C, Tungasukruthai S, Sritularak B, et al. Ephemeranthol A Suppresses Epithelial to Mesenchymal Transition and FAK-Akt Signaling in Lung Cancer Cells. *Anticancer Research*. 2020;40(9):4989-99.
105. Pinkhien T, Petpiroon N, Sritularak B, Chanvorachote P. Batatasin III inhibits migration of human lung cancer cells by suppressing epithelial to mesenchymal transition and FAK-AKT signals. *Anticancer research*. 2017;37(11):6281-9.
106. Rahman MA, Ramli F, Karimian H, Dehghan F, Nordin N, Mohd Ali H, et al. Artonin E induces apoptosis via mitochondrial dysregulation in SKOV-3 ovarian cancer cells. *PLoS one*. 2016;11(3):e0151466.
107. Zhou X, Zhou R, Li Q, Jie X, Hong J, Zong Y, et al. Cardamonin inhibits the proliferation and metastasis of non-small-cell lung cancer cells by suppressing the PI3K/Akt/mTOR pathway. *Anti-Cancer Drugs*. 2019;30(3):241-50.
108. Agarwal E, Brattain MG, Chowdhury S. Cell survival and metastasis regulation by Akt signaling in colorectal cancer. *Cellular signalling*. 2013;25(8):1711-9.
109. Wang S, Yan Y, Cheng Z, Hu Y, Liu T. Sotetsuflavone suppresses invasion and metastasis in non-small-cell lung cancer A549 cells by reversing EMT via the TNF- $\alpha$ /NF- $\kappa$ B and PI3K/AKT signaling pathway. *Cell death discovery*. 2018;4(1):1-11.

110. Hay N. The Akt-mTOR tango and its relevance to cancer. *Cancer cell*. 2005;8(3):179-83.
111. Wu C, Qiu S, Liu P, Ge Y, Gao X. Rhizoma Amorphophalli inhibits TNBC cell proliferation, migration, invasion and metastasis through the PI3K/Akt/mTOR pathway. *Journal of ethnopharmacology*. 2018;211:89-100.
112. Lamouille S, Connolly E, Smyth JW, Akhurst RJ, Derynck R. TGF- $\beta$ -induced activation of mTOR complex 2 drives epithelial-mesenchymal transition and cell invasion. *Journal of cell science*. 2012;125(5):1259-73.
113. Gulhati P, Bowen KA, Liu J, Stevens PD, Rychahou PG, Chen M, et al. mTORC1 and mTORC2 regulate EMT, motility, and metastasis of colorectal cancer via RhoA and Rac1 signaling pathways. *Cancer research*. 2011;71(9):3246-56.
114. Codony-Servat J, Verlicchi A, Rosell R. Cancer stem cells in small cell lung cancer. *Translational lung cancer research*. 2016;5(1):16.
115. Nassar D, Blanpain C. Cancer stem cells: basic concepts and therapeutic implications. *Annual Review of Pathology: Mechanisms of Disease*. 2016;11:47-76.
116. Koren E, Fuchs Y. The bad seed: Cancer stem cells in tumor development and resistance. *Drug Resistance Updates*. 2016;28:1-12.
117. Srinual S, Chanvorachote P, Pongrakhananon V. Suppression of cancer stem-like phenotypes in NCI-H460 lung cancer cells by vanillin through an Akt-dependent pathway. *International journal of oncology*. 2017;50(4):1341-51.
118. Chantarawong W, Chamni S, Suwanborirux K, Saito N, Chanvorachote P. 5-O-Acetyl-Renieramycin T from Blue Sponge *Xestospongia* sp. Induces Lung Cancer Stem Cell Apoptosis. *Marine drugs*. 2019;17(2):109.
119. Xia P, Xu X-Y. PI3K/Akt/mTOR signaling pathway in cancer stem cells: from basic research to clinical application. *American journal of cancer research*. 2015;5(5):1602.
120. Matsui WH. Cancer stem cell signaling pathways. *Medicine*. 2016;95(Suppl 1).
121. Shibue T, Weinberg RA. EMT, CSCs, and drug resistance: the mechanistic link and clinical implications. *Nature reviews Clinical oncology*. 2017;14(10):611.
122. Singh A, Settleman J. EMT, cancer stem cells and drug resistance: an emerging axis of evil in the war on cancer. *Oncogene*. 2010;29(34):4741-51.
123. Thiery JP, Acloque H, Huang RY, Nieto MA. Epithelial-mesenchymal transitions in development and disease. *cell*. 2009;139(5):871-90.
124. Kharbanda A, Rajabi H, Jin C, Alam M, Wong K-K, Kufe D. MUC1-C confers EMT and KRAS independence in mutant KRAS lung cancer cells. *Oncotarget*. 2014;5(19):8893.

125. Huang Y, Chen Y, Mei Q, Chen Y, Yu S, Xia S. Combined inhibition of the EGFR and mTOR pathways in EGFR wild-type non-small cell lung cancer cell lines with different genetic backgrounds. *Oncology reports*. 2013;29(6):2486-92.
126. Guibert N, Ilie M, Long E, Hofman V, Bouhleb L, Brest P, et al. KRAS mutations in lung adenocarcinoma: molecular and epidemiological characteristics, methods for detection, and therapeutic strategy perspectives. *Current molecular medicine*. 2015;15(5):418-32.
127. Riely GJ, Marks J, Pao W. KRAS mutations in non-small cell lung cancer. *Proceedings of the American Thoracic Society*. 2009;6(2):201-5.
128. Arner EN, Du W, Brekken RA. Behind the wheel of epithelial plasticity in KRAS-driven cancers. *Frontiers in oncology*. 2019;9:1049.
129. Xia R, Xu G, Huang Y, Sheng X, Xu X, Lu H. Hesperidin suppresses the migration and invasion of non-small cell lung cancer cells by inhibiting the SDF-1/CXCR-4 pathway. *Life sciences*. 2018;201:111-20.
130. Lv X-q, Qiao X-r, Su L, Chen S-z. Honokiol inhibits EMT-mediated motility and migration of human non-small cell lung cancer cells in vitro by targeting c-FLIP. *Acta Pharmacologica Sinica*. 2016;37(12):1574-86.
131. Chen M, Hu C, Guo Y, Jiang R, Jiang H, Zhou Y, et al. Ophiopogonin B suppresses the metastasis and angiogenesis of A549 cells in vitro and in vivo by inhibiting the EphA2/Akt signaling pathway. *Oncology reports*. 2018;40(3):1339-47.
132. Chanvorachote P, Chamni S, Ninsontia C, Phiboonchaiyanan PP. Potential anti-metastasis natural compounds for lung cancer. *Anticancer Research*. 2016;36(11):5707-17.



จุฬาลงกรณ์มหาวิทยาลัย  
**CHULALONGKORN UNIVERSITY**

## VITA

**NAME** Kittipong Sanookpan

**DATE OF BIRTH** 5 April 1997

**PLACE OF BIRTH** Ubon Ratchathani

**INSTITUTIONS ATTENDED** Inter-Department of Pharmacology

**PUBLICATION** Sanookpan K, Nonpanya N, Sritularak B, Chanvorachote P. Ovalitenone Inhibits the Migration of Lung Cancer Cells via the Suppression of AKT/mTOR and Epithelial-to-Mesenchymal Transition. *Molecules*. 2021; 26(3): 638.  
[doi.org/10.3390/molecules26030638](https://doi.org/10.3390/molecules26030638)